BEST AVAILABLE IMAGES

Defective images within this document are accurate representations of the original documents submitted by the applicant.

Defects in the images may include (but are not limited to):

- BLACK BORDERS
- TEXT CUT OFF AT TOP, BOTTOM OR SIDES
- FADED TEXT
- ILLEGIBLE TEXT
- SKEWED/SLANTED IMAGES
- COLORED PHOTOS
- BLACK OR VERY BLACK AND WHITE DARK PHOTOS
- GRAY SCALE DOCUMENTS

IMAGES ARE BEST AVAILABLE COPY.

As rescanning documents *will not* correct images, please do not report the images to the Image Problem Mailbox.

REMARKS

The paragraphs of the outstanding Office Action are responded to as follows:

Claim 1 has been amended to include the limitations of claims 2 through 5 in order to help clarify the invention scope. The claims have been narrowed to be more specific about the arrangement of the imaging component that is effective to provide a compensated "Vertically Aligned" cell. Figure 8 shows an arrangement of claim 1 with two positively birefringent layers on a negative base. Claim 15 has been amended to reflect a compensation film comprising two positive birefringent materials on a negative base and claims 16 and 17 have been amended accordingly.

Claims 1 stands rejected under 35 U.S.C. 103(a) as being unpatentable over Applicant admitted prior art (AAPA) in view of US 6,034,756 (Yuan et al) and Xu (US 5,638,200. According to the Examiner, AAPA, Fig 4A herein, shows a vertially aligned cell with a polarizer and a positively birefringent material. The Examiner then turns to Yuan as showing a compensating layer (180) in Fig. 5 having an optic axis normal to to the LC cell substrate and suggesting a tilt to improve the compensation of a twisted Nematic (TN) cell.

Clearly, Fig. 4A does not show the optic axis being tilted in a plane perpendicular to the liquid crystal cell face. The optic axis of the compensation film 27 in the AAPA prior art lies in or parallel to the surface of the liquid crystal cell, which is different from the present invention in which the optic axis of the positive birefringent material is tilted in a plane that is perpendicular to the liquid crystal cell face. The optic axis of the compensation film 27 in the prior art does not tilt in a plane that is perpendicular to the liquid crystal cell face (this plane will be the one determined by the z-axis and the optic axis of the compensation ffilm 27).

Yuan shows a tilted layer but it is a discotic negatively birefringent layer and is employed with a TN cell. As demonstrated in the attached Declaration and enclosures, there is not equivalence between means of compensating for various tpes of LC cells. In order for this negative birefringent material to compensate for the TN LCD, the change in optic axis is designed to mimic to some degree the tilt of the directors in the LC cell (Col.3, lines 36-38).

This disclosure does not suggest the use of two layers of a positively birefringent material disposed on a negatively birefringent base as a compensator for a vertically-aligned LCD. As a matter of fact, the change in optic axis of the positive birefringent material in examples 1-3 (page 12, line 25- page 13, line 14 of this application) do not and cannot mimic the tilt of the directors in the LC cell.

The Xu reference relates to a twisted LC cell (col. 6, lines 16; claim 1) and, like Yuan, has limited significance as a teaching instrument for a vertially aligned cell.

Enclosed herewith is a Declaration of inventor Xiang Dong Mi. The Declaration provides further basis to demonstate why the combination of the invention is not obvious including the authority provided by the extracts from the Lueder reference.

To summarize, the Examiner is attempting to combine combinations of references which cannot appropriately be combined because they are directed to specific display features different from those of the present claims. The Examiner is attempting to create a prior art mosaic by extracting small pieces of disclosure from different references when one of ordinary skill in the art would know that compensation films used for one type of LC cell cannot be applied to another type of cell. Applicants have provided ample evidence in authority and Declaration form that the compensation solutions for different types of LC cells are different and not obvious over each other. "Obvius to try" is not a valid basis for rejection. The Examiner has not provided any motivation in the art to arrive at the present invention as opposed to the relatively ineffective results of the admitted prior at.

In view of the foregoing amendments and remarks, the Examiner is respectfully requested to withdraw the outstanding rejections and to pass the subject application to Allowance.

Respectfully submitted,

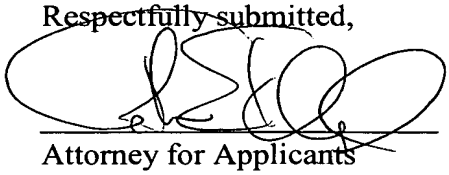

Attorney for Applicants
Registration No. 25,518

Arthur E. Kluegel/dlm
Rochester, NY 14650
Telephone: (585) 477-2625
Facsimile: (585) 477-1148

83664AEK
Customer No. 01333

IN THE UNITED STATES PATENT AND TRADEMARK OFFICE

In re Application of:

Xiang-Dong Mi, et al

VERTICALLY ALIGNED LIQUID CRYSTAL IMAGING COMPONENT WITH COMPENSATION LAYER

Serial No. 10/020,543

Filed 30 November 2001

Group Art Unit: 2871

Examiner: Zhi Qiang Qi

I hereby certify that this correspondence is being deposited today with the United States Postal Service as first class mail in an envelope addressed to Commissioner For Patents, P.O. Box 1450, Alexandria, VA 22313-1450.

Deidra L. Mack

Deidra L. Mack

July 21, 2004

Date

Commissioner for Patents
P.O. Box 1450
Alexandria, VA. 22313-1450

Sir:

DECLARATION UNDER RULE 132

The undersigned, Xiang-Dong Mi, of Rochester, New York, declares that:

He has received the degree of B.S. in Physics from Beijing Normal University (1992) and a PhD in Chemical Physics from Kent State University (2000);

He has been employed as a scientist with Eastman Kodak Company in the area of optical products since 2000 and has been involved in the study of physics for over 16 years;

He is an inventor in the above-captioned patent application;

He has reviewed the outstanding Office Action and any applicable cited references;

In particular, he notes that the Examiner has disputed the inventors position that it is well known in the art that compensation films for different modes of liquid crystals are not compatible and that a Twisted Nematic (TN) cell is aligned differently and operates on a different optical principle from a vertically aligned cell, and therefore the optical properties required to compensate the two

are not the same. The Examiner cites Yuan '756 and Xu '200, as evidence that this incompatibility does not exist.

The term "compatibility" as used herein refers to optical performance, not physical placement. One can physically combine a particular compensator with a particular LC cell but the results show that it simply does not work. This is what is meant when the inventors state that: "compensation films for different modes of liquid crystals are not compatible". It seems that Examiner misunderstood what was intended by the term "compatibility". The isocontrast plots or Viewing Angle Characteristic plots (VAC) show the compatibility issue.

In general, one compensation film designed for one type of liquid crystal mode does not work well or equally well for another type of liquid crystal mode. In particular, the compensator designed for a Twisted Nematic LC, does not work equally well when it is applied to a vertically aligned LC. This statement can be supported by the book "Liquid Crystal Displays" by Ernst Lueder (John Wiley & SONS, Ltd, 2001). Chapter 6 "Propagation of light with an arbitrary incident angle through anisotropic media" reviews compensators for various LCD modes. The copy of Chapter 6 and other pertinent portions are enclosed herewith.

Pages 11-16 describe the operation of a TN cell. Pages 43-4 describe a vertically aligned cell (also known as a DAP cell). Pages 55-56 show the propagation of light through a Twisted Nematic) TN cell. Pages 105-111 describe pair-wise use of negative compensators to compensate for a positively birefringent cell.

Page 105, the last line provides "Measures against degraded contrast and the associated changes for an increased viewing angle are compensation foils with negative birefringence, adding an inverse cell with negative or positive birefringence and the in-plane switching mode (IPS); the gray scale inversion is avoided by multi-domain pixels, IPS and by foils with positive birefringence" indicates that the compensation foils (or compensators) are different for different LCD modes.

Page 108, last paragraph, provides "The compensation discussed so far was based on vertically aligned LC molecules in Figure 6.7. In TN cells, however, the molecules close to the two orientation layers stay aligned with directors parallel to the surface of the glass plates and perpendicular to each other"

confirms that the compensator for a vertically aligned LC is different from the compensator for a TN aligned LC.

Page 114, first paragraph under section 6.3, provides "So far we have investigated viewing angle limitation and problems with gray shades in TN cells." The author notes that a basic cause for shortcomings varies depending on the type of LC cell. The major TN shortcoming does not show up in displays with non-twisted arrangements such as In-Plane Switching (IPS) or in a π (OCB or Bend) cell and also indicates that the compensator for a TN is different from the compensator for other LCDs, such as IPS, and bend aligned LCD. Vertically aligned cells are non-twisted displays.

The examples of compensators for a TN are discussed referring to Figure 6.12 and Figure 6.13 on Pages 110 and 111. The examples of compensators for STN are discussed referring to Figure 6.15 and Figure 6.16 on Pages 112 and 113. The first paragraph on Page 117 discusses the compensation of IPS referring to Figure 6.20.

Bend aligned cells (or OCB, or π-cells) are discussed on Pages 117-119; for example, "the OCB cell also exhibits a wide viewing angle" on Page 117, and, "The viewing angle can be further enhanced by adding a negatively birefringent compensation foiled with the self-compensating director configuration" (first paragraph, Page 119).

Compensators are not typically useful regardless of the type or mode of LC employed. For each LCD mode, there are various ways of compensating the LC. Some ways are superior to others in terms of viewing angle, manufacturability, package, material choices, and so on.

Turning to the Examiner's reliance on Yuan, (U.S. Patent 6,034,756), Yuan states

> One of ordinary skill in the art would appreciate from this specification that other twist orientations, modes, types of LC cells and types of LC material could be used. For example, ferroelectric liquid crystal (FLC) cells, supertwisted-nematic (STN) cells, optical compensated bend cells, pi-cells, and homeotropic (perpendicular) alignment LC cells could also be used (Col. 4, lines 57-64).

This statement refers to Fig. 8, where ref 220 is the compensator without any specifics, and ref. 230 is the LC cell, also without specifics. Thus the statement is true because it says nothing about the suitability of any particular compensators for particular cells; it does not say that any particular compensator 220 may be generically employed for different types of LCs.

Yuan continues the teaching according to the compensation principle that is used according to his invention, that "the compensating layer 220 has **negative** birefringence (i.e., $n_e < n_o$) and the absolute value of $\Delta n'$ equals the absolute value of Δn. Thus, the compensating layer 220 has negative birefringence and a right-hand twist" (col. 5, lines 19-20). He also states that "the LC cell has **negative** birefringence and the compensating layer has **positive** birefringence" (col.5, lines 21-23). Contrary to this teaching and according to Applicant's invention, the claimed compensator has **positive** birefringence, and the bend aligned LC also has **positive** birefringence. The structure of the compensator does not mimic the structure of the bend aligned LC as suggested by Yuan and this design is thus counter intuitive and was not obvious to me at the time of invention

Applicants agree that "an optical compensator of some type be inserted in twisted nematic, super twisted nematic, optically compensated bend, in-plane switching, or vertically aligned liquid crystal displays" to widen the viewing angle of liquid crystal displays. But the same optical compensator does not compensate all of the liquid crystal displays, for the reasons discussed above. It would not obvious to me or, in my opinion, to others skilled in the art that a compensator arrangement for one type of cell would be expected to be useful for another type of cell.

As further evidence that particular compensators must be developed for particular cells, the compensation principle of Lueder and Yuan is based on the use of a compensator with negative birefringence to compensate for a LC with positive birefringence, and the compensator mimics the structure of the LC is well known.

The Examiner cited reference Xu (U.S. 5,638,200) as evidence to show using a positively birefringent material as the compensation film is common knowledge in the art. Xu however teaches the use of a positive birefringent

material to compensate a twisted nematic (TN) LCD, and he does not discuss anything about a vertically aligned LCD nor the use of a positively birefringent material to compensate a vertically aligned LCD. Neither Yuan nor Xu suggests nor provides motivation to arrive at the compensation arrangement of the invention.

The design of the present invention is counter intuitive to the conventional teachings.

In view of the foregoing facts, it would not have been obvious to me from the art relied on by the Examiner to arrive at the particular compensator/LC cell claimed from the art referred to above at the time the invention was made.

The undersigned declares further that all statements made herein of the undersigned's own knowledge are true and all statements made on information and belief are believed to be true. These statements are made with the knowledge that willful false statements and the like so made are punishable by fine or imprisonment, or both, under section 1001 of Title 18 of the United States Code and that such willful false statements may jeopardize the validity of the application or any patent issuing thereon.

Xiang-Dong Mi

Date: 7/21/2004

Enclosure

Excerpts from Liquid Crystal Displays
by Ernst Lueder

Liquid Crystal Displays

ADDRESSING SCHEMES AND ELECTRO-OPTICAL EFFECTS

Ernst Lueder
University of Stuttgart, Germany

JOHN WILEY & SONS, LTD
Chichester • New York • Weinheim • Brisbane • Singapore • Toronto

Contents

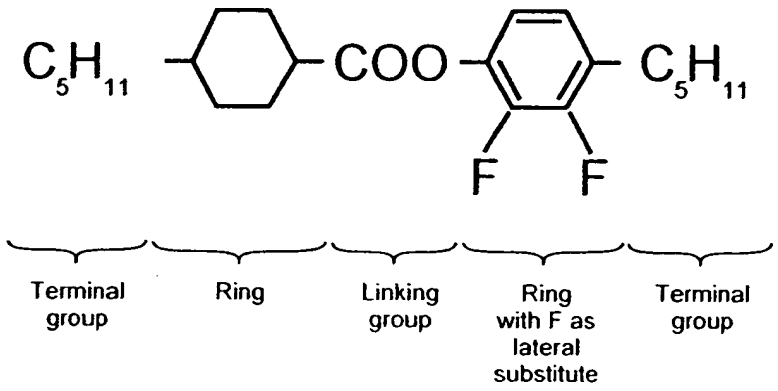

Figure 2.8 The basic structure of a calamitic LC molecule

Table 2.2 Properties of nematic LC materials with a wide temperature range

	MLC-1380000	MLC-13800100	MLC-1390000	MLC-13900100
Transition temp. smectic-nematic	$< -40°C$	$< -40°C$	$< -40°C$	$< -40°C$
Clearing pt T_c	110°C	111°C	110.5°C	110.5°C
Rotational viscosity, 20°C	228 mPas	151 mPas	235 mPas	167 mPas
$\Delta\epsilon$ 1 kHz, 20°C	+8.9	+5.0	+8.3	+5.2
$n_0 = n_\perp$	1.4720	1.4832	1.4816	1.4906
$n_e = n_\parallel$	1.5622	1.5735	1.5888	1.5987
Δn	+0.0902	+0.0903	+0.1073	+0.1081

2.2 The Operation of a Twisted Nematic LCD

The liquid crystals used are calamitic and thermotropic in the nematic phase. The operation of this most widely applied LCD will be phenomenologically described in order to give an overview over the entire flat panel display system, including the addressing scheme (Demus *et al.*, 1998a; Kaneko, 1987; Lueder, 1998a). This alleviates the more analytical and detailed treatments which follow.

2.2.1 The electro-optical effects in transmissive twisted nematic LC-cells

Figure 2.9 depicts the top view of a display panel with the conducting rows and columns terminating in the contact pads. The rectangular pixels can only be electrically addressed from those contact pads.

A colour VGA display, as used in laptops, has 480 rows and 3 × 320 columns forming triple dots for the three colours red, green and blue. An NTSC TV display has 484 rows and 3 × 450 columns corresponding to 653 400 pixels, whereas an HDTV display has

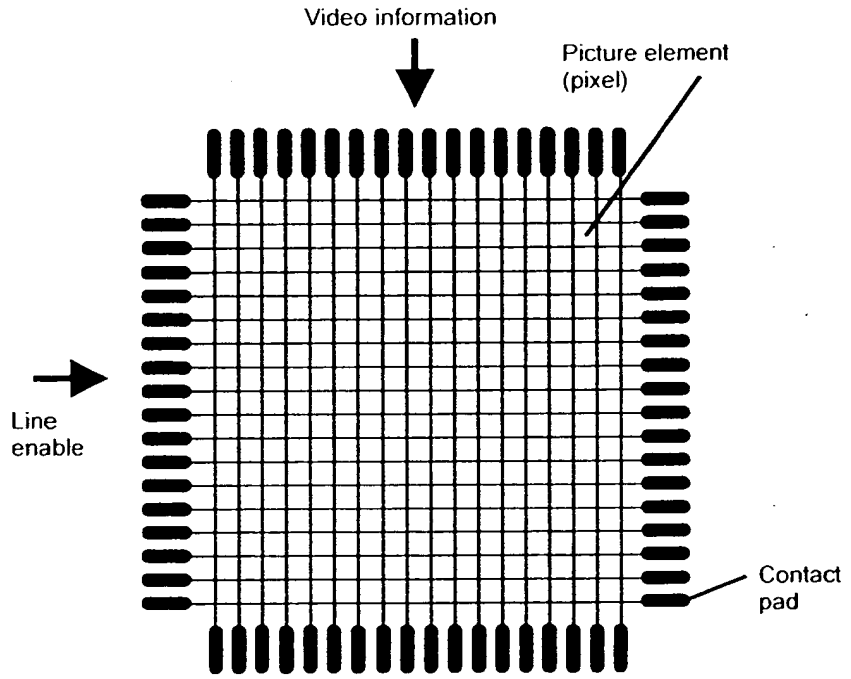

Figure 2.9 Top view of the rows, columns, pixels and contact pads of a display panel

$1080 \cdot 3 \cdot 1920 = 7\,320\,800$ pixels. For more standardized formats, see the table in Appendix 1.

Figure 2.10 shows a pixel of a transmissive twisted nematic LC-cell with no voltage applied. The white back light *f* passes the polarizer *a*. The light leaves it linearly polarized in the direction of the lines in the polarizer, and passes the glass substrate *b*, the transparent electrode *c* out of Indium-Tin-Oxide (ITO) and the transparent orientation layer *g*. This layer, made of an organic material such as polyimide, 100 nm thick, is rubbed to generate grooves in the direction of the plane of the polarized light. In these grooves the rod-like LC molecules are all anchored in parallel, but, as shown in Figure 2.11, with a pretilt angle α_0 to the surface of the orientation layer. The sequence of layers is the same on the second glass plate. A typical thickness of the cell in Figure 2.10 is $d = 3.5\,\mu$ to $4.5\,\mu$. The grooves on the second plate are perpendicular to those on the first plate. This forces the liquid crystal molecules to twist on a helix by $\beta = 90°$ from one plate to the other without the addition of chiral compounds. All twist angles are called β.

Due to the birefringence, the components of the electric field vector of the light in parallel and perpendicular to the directors travel with different speeds, which depend up-on the wavelength. They superimpose along their path between the two glass plates first to elliptically polarized light, in the distance $d/2$ from the input to circularly polarized light, then again to an elliptic polarization, and if

$$d = \frac{\sqrt{3}}{2} \frac{\lambda}{\Delta n} \tag{2.15}$$

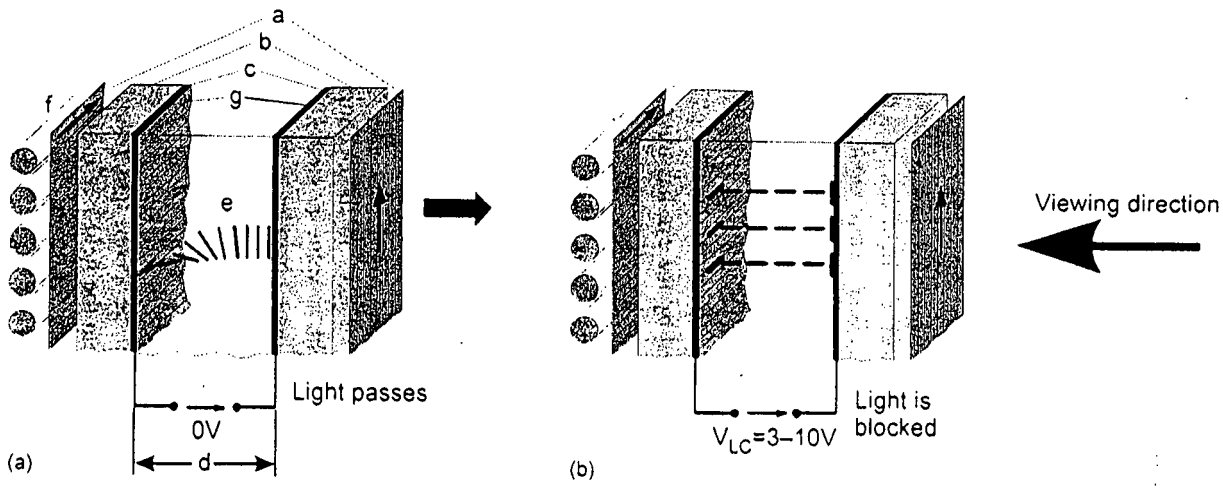

Figure 2.10 The structure of a TN-LCD (a) while light is passing, and (b) while light is blocked. a: polarizer; b: glass substrate; c: transparent electrode; g: orientation layer; e: liquid crystal; f: illumination

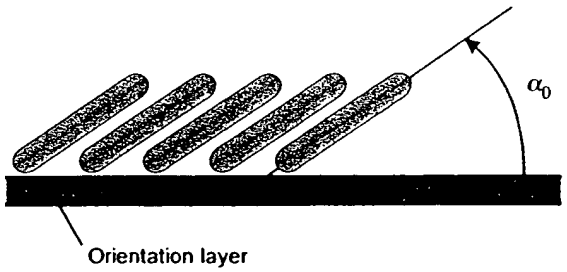

Figure 2.11 LC molecules with pretilt angle α_0 on top of the orientation layer

they reach the analyser again linearly polarized, but with the polarization plane rotated by 90°. If the analyser is crossed with the polarizer, the light can pass the analyser. The pixel appears white. This operation is termed the *normally white mode*. If the analyser is rotated by 90°, a parallel analyser, the light is blocked in the analyser. The pixel is black. This is called the *normally black mode*. A useful visualization of what happens to the light while travelling through the cell is as follows: the planes of the various polarizations follow the twist of the helix. This is, however, only true if Equation (2.15) holds. The explanation is also only true for light travelling and viewed perpendicular to the plane of the substrate. If viewed under a different angle, light perceived by the eye has travelled in a different path with different angles to the director and a different cell thickness d.

If a voltage V_{LC} of the order of 2 V is applied across the cell, as shown in Figure 2.10(b), using the two transparent ITO-electrodes 100 nm thick, the resulting electric field attempts to align the molecules for $\Delta\varepsilon > 0$ parallel to the field. This holds independent of the sign of the vector of the electrical field, as already pointed out in Section 2.1.2. Hence, the following effects are not dependent on the polarity of V_{LC}. Due to the anchoring forces, a thin LC layer on top of the orientation layers maintains its position almost parallel to the surfaces. A threshold voltage V_{th} is needed to overcome intermolecular forces before the twisted molecules start to rotate. A uniform start over the plane of the panel is favoured by a pretilt angle around 3°, which seems to avoid strong differences in the anchoring forces. Only at a saturation voltage V_{max} several times V_{th} with a value around 10 V have all molecules besides those on top of the orientation layers aligned parallel to the electric field, as depicted in Figure 2.10(b). In this state the vector of the electrical field of the incoming light oscillates perpendicular to the directors, and encounters only the refractive index $n_\perp$. Hence, no bi-refringence takes place and the wave reaches the crossed analyser in the same linearly polarized form as at the input. The analyser blocks the light and the pixel appears black. This is an excellent black state as it is independent of the wavelength, resulting in a blocking of the light. This black state is gradually reached from the field-free initial state by increasing the voltage V_{LC} from OV over an intermediate voltage up to V_{max}, which is also gradually rotating the molecules in Figure 2.12 from the initial twisted state with directors parallel to the surfaces (Figure 2.10(a)) over an intermediate state with the director already tilted down with tilt angle α (Figure 2.12(b)) to the final state with directors parallel ($\alpha = 90°$) to the electric field. The transmitted luminance, also termed *transmittance*, of the light is shown in Figure 2.13 for the normally white mode discussed so far. In the normally black mode, the analyser is parallel to the polarizer and allows the light to pass at the voltage

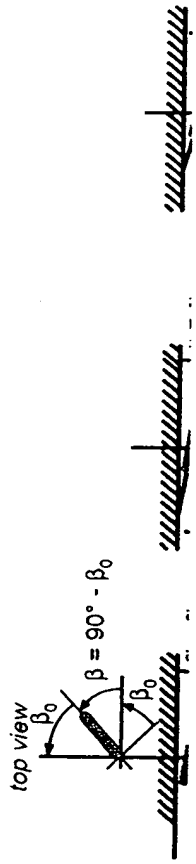

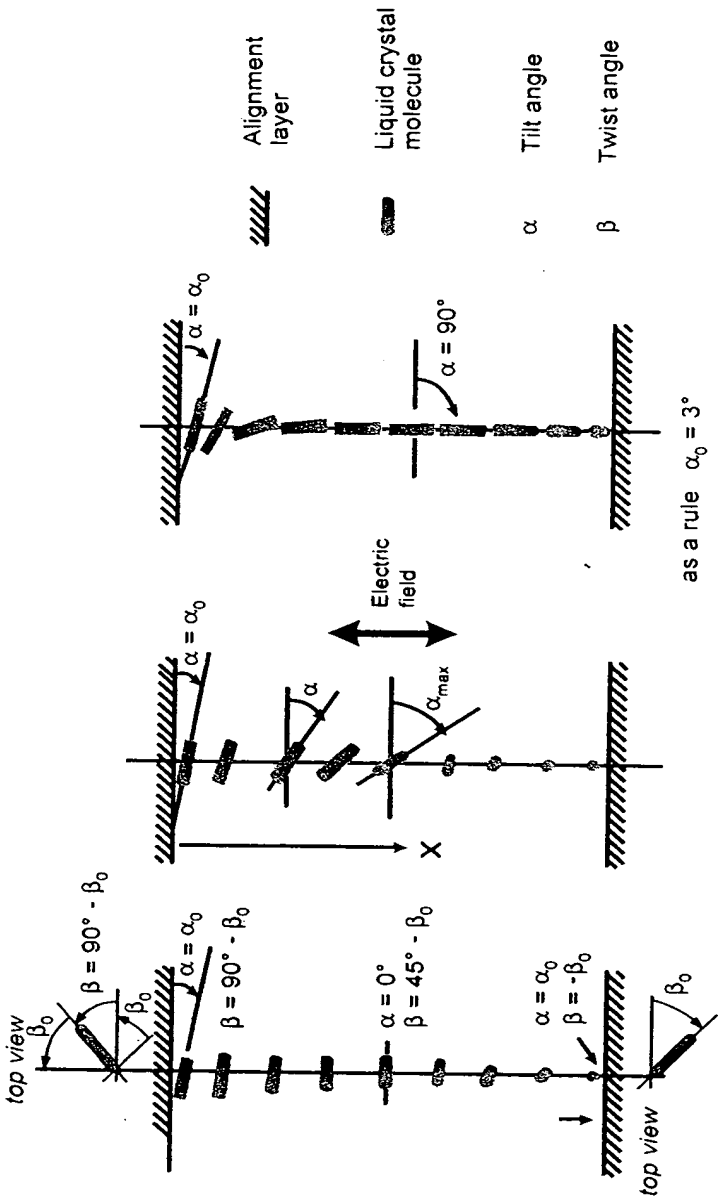

Figure 2.12 Change in the position of the LC molecules with increasing voltage

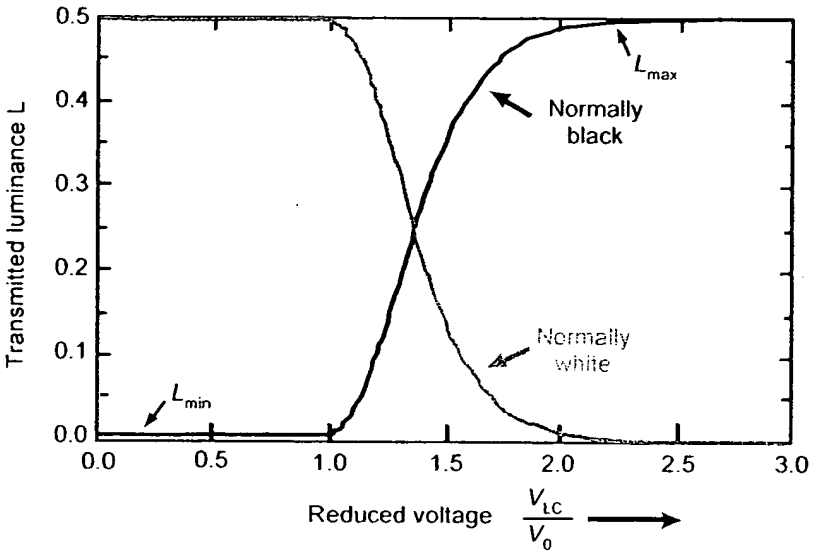

Figure 2.13 Transmitted luminance versus the reduced voltage V_{LC} across the LC cell for the normally white and normally black modes

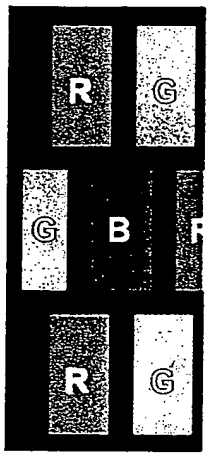

(a)

Figure 2.14 The ge
triangles. (b) in stri

$V_{th} \leq V_{LC} \leq V_{max}$. For this mode the transmitted luminance is also depicted in Figure 2.13. Only in this mode is the threshold voltage V_{th} visible, as in the normally white mode a small change in luminance at a high value of the luminance cannot be perceived by the eye.

Luminance is the correct term for 'brightness'. The physical meaning and dimensions of luminance and other display-related units are explained in Appendix 2.

The blocking of light in the analyser as described by Equation (2.15) is only valid for one wavelength for which, as a rule, yellow light with $\lambda = 505\,\text{nm}$ is chosen. As other wavelengths can still pass the analyser, the black state is not perfect. As a rule, it has a bluish tint. The imperfect black state can be improved by compensation foils, as discussed later.

The Contrast Ratio CR of a display is defined by

$$CR = \frac{\text{highest luminance in the pixels, } L_{max}}{\text{lowest luminance in the pixels, } L_{min}} \tag{2.16}$$

The measurement should be performed without the interference of reflected ambient light, i.e. in darkness. If the black state in the denominator of Equation (2.16) is increased by the imperfect blocking of the light, contrast falls in any case. This is the case in the normally black state, whereas the normally white state described above yields an excellent contrast due to a much lower value of the denominator in Equation (2.16).

Grey shades of a pixel are controlled by the voltage V_{LC} in Figure 2.13, which modulates the luminance from a full but imperfect black up to a full white. Luminance differs when the display is viewed under angles different from perpendicular to the glass plates. Contrast decreases the more oblique the angles become.

The TFT addressing circuit will be placed on the glass next to the backlight in Figure 2.10. In a colour display, the glass plate facing the viewer carries the pixellized colour filter,

shown in Figure 2.
absorbs all wavel
respectively. The
voltage V_{LC} in the

The geometrical
diagonals in Figur
stripes in Figure
graphs.

The cross-sectic
and B, an absorpt
matrix, an overcoa
over the entire di
unstructured. The
prevents light betv
electrodes nor exh
lighten up the blac
suitable material f
reflectivity of onl
40 percent. The o
different heights o

2.2.2 *The addre*

So far we know th
the appropriate pix

For $\alpha = \pi/2$ the linearly polarized light in Figure 3.15 always encounters the refractive index $n_\perp$ independent of the tilt, and hence is independent of V (curve 7 in Figure 3.16), which is of no use for a phase shifter.

3.2.5 *The DAP cell or the vertically aligned cell*

The cell operating with the deformation of aligned phases, called the DAP cell (Glueck, 1995), is the inverse of the Fréedericksz cell. In the field-free state the LC molecules are perpendicularly (or in other words, homeotropically) aligned to the surface of both substrates, as depicted in Figure 3.17. This cell is also called a Vertically Aligned (VA) LCD. In this situation, incoming linearly polarized light with a wave vector $\vec{k}$ in parallel to the z-axis in Figure 3.17 does not encounter birefringence, and arrives at the second substrate with an unchanged state of its polarization. If the analyser is parallel to the polarizer, the full light can pass representing the normally white state. If the analyser is crossed with the polarizer, the light is blocked at the output for all wavelengths and independent of d. This is the normally black state. The cell exhibits an extremely good black state, since the blocking is again independent of λ. Further, the molecules on the orientation layer are also, contrary to the Fréedericksz cell, vertically aligned. A low black value in the denominator of the contrast in Equation (3.82) is most beneficial for a high contrast. The main attraction of the DAP cell is this extremely high contrast, reaching values of more than 500 : 1.

If an electrical field is applied, the LC molecules orient themselves perpendicularly to the field as $\Delta\varepsilon < 0$. This alignment corresponds to the same alignment of the Fréedericksz cell

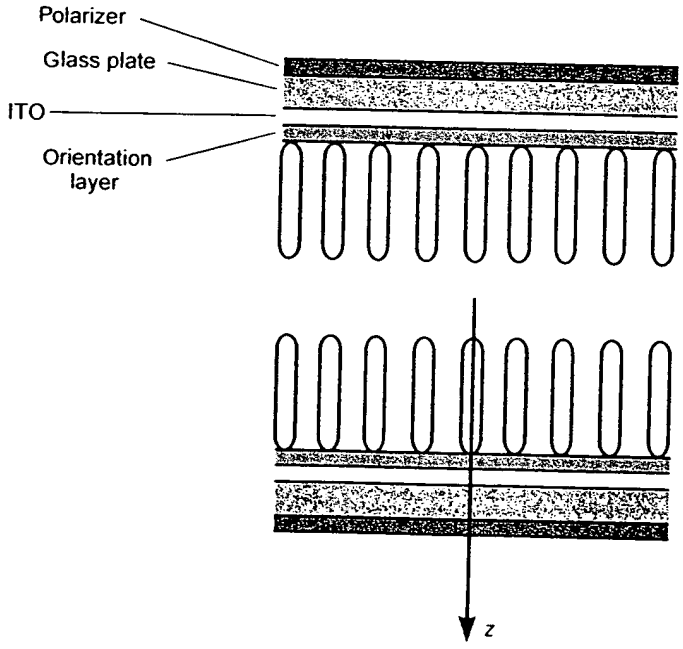

Figure 3.17 The DAP cell or Vertically Aligned (VA) cell in the field-free state

in the field-free state. Hence, all results in Equations (3.40) through (3.87) also apply to the DAP cell which is exposed to an electric field. The DAP cell is as well suited for phase-only modulators, as the pertinent Equations (3.90) and (3.95) also hold if a voltage V is applied. However, for the voltage-dependent refractive index $n(V)$, we obtain $n(V) \in \lfloor n_{\parallel}, n_{\perp} \rfloor$, but contrary to the Fréedericksz cell with $n_{\perp}$ for the lower voltage and $n_{\parallel}$ for the higher voltage. The homeotropic alignment of the molecules in the DAP cell requires special care. It is achieved by a spin-coated monomolecular silane-layer disolved in ethyl alcohol which is polymerized in the presence of humidity. The high polarity of silane thus generated anchors the polar LC molecules perpendicular to the surface. If a voltage is applied, all molecules are supposed to tilt in the same direction, since they have to end up all in parallel to each other and parallel to the plane of the substrates. This is realized by a small uniformly oriented pretilt of around 1° to 2° off the normal of the surface. A larger pretilt must be avoided, since it degrades the black state. The polymerized silane layer is uniformly rubbed with a carbon fibre brush to generate the grooves for the orientation of the molecules. As an alternative, this pretilted uniform orientation is produced with a very high manufacturing yield by a SiO_2 layer obliquely evaporated or sputtered under an angle of 2° off the normal. This alternative also achieves a very high contrast exceeding 500 : 1. The sputtering of this SiO_2 layer is explained in Figure 3.18. The DAP cell is, like a Fréedericksz cell, designed as a $\lambda/2$-plate with a retardation $\Delta nd = \lambda/2$, and hence $d = \lambda/2\Delta n$. For most commercially available LC materials exhibiting $\Delta n = 0.08$, this leads for $\lambda = 550$ nm to a cell thickness of $d = 3.4$ µ. The reflective version is a $\lambda/4$-plate with a thickness of $d = 1.7$ µ, which is often too thin for a high yield fabrication because small particles could easily cause shorts. The search for electro-optical effects with a larger cell thickness leads to the HAN cells and the Twisted-Nematic cells (TN-cells), which are covered in the next chapter and in Chapter 4.

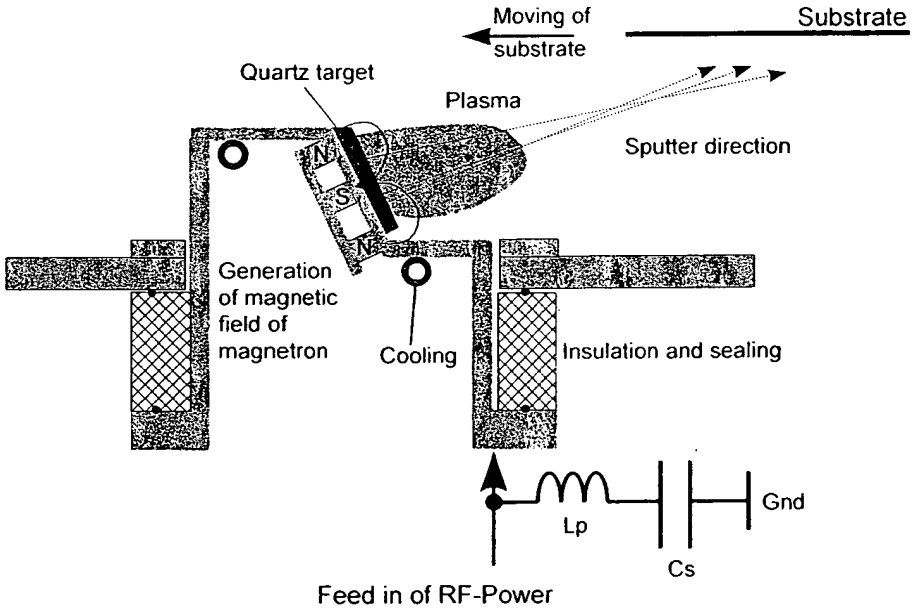

Figure 3.18 The sputtering of an SiO_2 orientation layer under an oblique angle of 70°

A reflective DAP cell with a thickness $d/2$ can be constructed in the same way as a Fréedericksz cell.

3.2.6 The HAN cell

The Hybrid Aligned Nematic cell (HAN cell) represents a mixture between the Fréedericksz cell and the DAP cell (Glueck, 1995). We investigate the reflective version in Figure 3.19(a), because among untwisted cells they have turned out to be more important. On the plate with the polarizer the LC molecules are in the field-free state in Figure 3.19(a) oriented all in the same direction parallel to the surface of the plate like in a Fréedericksz cell, whereas on the plate with the mirror they are homeotropically oriented. The linearly polarized light enters the cell at an angle $\alpha \neq 0$ to the x-axis, as in the transmissive and reflective Fréedericksz cells. The optical anisotropy Δn changes with z described by $\Delta n(z)$. At $z=0$ the light wave encounters the full anisotropy Δn, meaning that $\Delta n(0)=\Delta n$. This is only true for $\alpha \neq 0$. At $z=d$ the light encounters no anisotropy as the medium is isotropic with a refraction index $n_\perp$, reflecting in $\Delta n(d)=0$. Assuming a linear change of $\Delta n(z)$ we obtain $\Delta n(z)$ in Figure 3.19(b), leading to an effective retardation R of

$$R = \int_0^d \Delta n(z)dz = \frac{1}{2}\Delta nd. \tag{3.96}$$

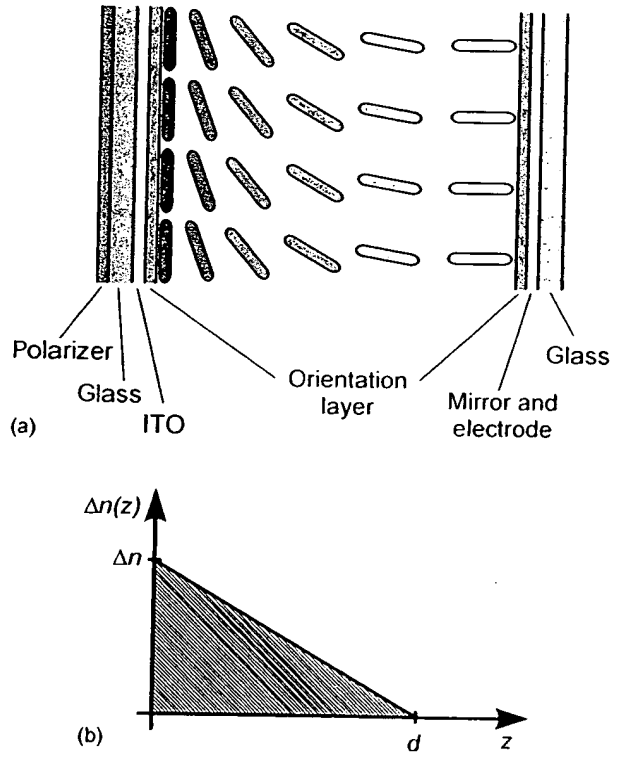

Figure 3.19 The reflective HAN cell. (a) Cross-section; (b) optical anisotropy $\Delta n(z)$

4 Electro-optic Effects in Twisted Nematic Liquid Crystals

4.1 The Propagation of Polarized Light in Twisted Nematic Liquid Crystal Cells

The Twisted Nematic cell (TN cell) is the most widely commercially used LC cell. It was proposed by Schadt and Helfrich (1971), and is therefore also termed the Schadt–Helfrich cell. The theoretical investigation is based on Jones' vectors. Solutions for the light exiting a TN cell were given by Yeh (1998), Yeh and Gu (1999), Grinberg and Jacobson (1976) and Rosenbluth *et al.* (1998). The derivation relies on rotating back the coordinate system to the original coordinates in twisted media and on the Chebychev identity of matrices (Bodewig, 1959). On the other hand, the derivation of the results presented here rotates the coordinates with the twist of the layers. The further calculation is based on Specht (2000).

The planar wave with wave vector $\vec{k}$ at the input of the cell propagates along the z-axis in Figure 4.1. We investigate the propagation through the cell without considering the light reflected at the LC molecules or absorbed in the cell. The incoming light is linearly polarized in the ξ-direction at an angle α to the x-axis with the electrical field $E_{\xi 0}$ giving the Jones vector

$$J_1 = \begin{pmatrix} J_x \\ J_y \end{pmatrix} = R(-\alpha) \begin{pmatrix} E_{\xi 0} \\ 0 \end{pmatrix} \tag{4.1}$$

in the x-y-coordinates. The LC molecules in the x-y-plane are all anchored in the rubbing grooves parallel to the x-direction. The directors of all molecules in the cell are parallel to the x-y plane and form a helix with the z-direction as the axis, and with the linear

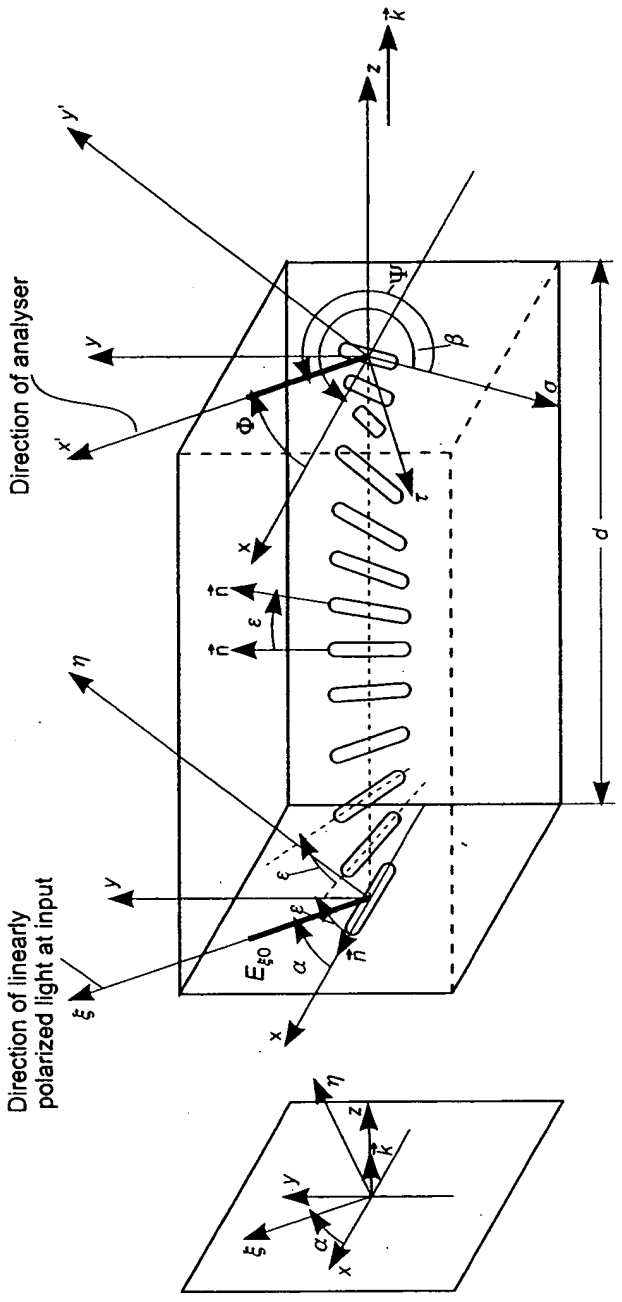

Figure 4.1 The general twisted nematic LCD with twist angle β

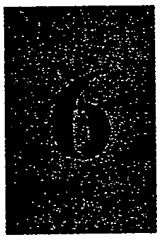

Propagation of Light with an Arbitrary Incident Angle through Anisotropic Media

6.1 Basic Equations for the Propagation of Light

In Chapters 3 and 4 we treated the case of incident light with a wave vector k parallel to the z-axis in Figure 4.1. This direction was for both the untwisted and twisted case in the field-free state perpendicular to the director $\vec{n}$ on the alignment layer. The more complex case is an arbitrary angle of incidence of light with respect to the director, as shown in Figure 6.1. The medium is anisotropic, meaning that the relative dielectric constant ε_{ij} and the refractive indices n_{ij} depend upon the direction, e.g. measured in orthogonal coordinates x, y and z. We assume, however, that the medium is homogeneous in layers with parallel plane borders. It is possible to find principal coordinates x', y' and z' in Figure 6.1 in which the tensor ε of the dielectric constants exhibits only zeros off the main diagonal given by

$$\varepsilon = \begin{pmatrix} \varepsilon_{x'} & 0 & 0 \\ 0 & \varepsilon_{y'} & 0 \\ 0 & 0 & \varepsilon_{z'} \end{pmatrix} = \begin{pmatrix} n_{x'}^2 & 0 & 0 \\ 0 & n_{y'}^2 & 0 \\ 0 & 0 & n_{z'}^2 \end{pmatrix}. \tag{6.1}$$

The relation between the permittivity and the refractive index was introduced in Equation (2.6).

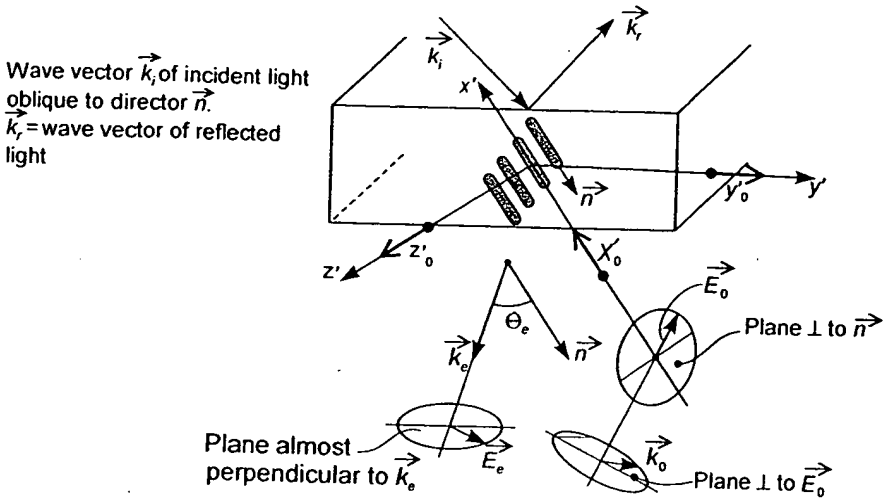

Figure 6.1 The direction of $\vec{k}_0$ and $\vec{E}_0$ of the ordinary beam and of $\vec{k}_e$ and $\vec{E}_e$ of the extraordinary beam in a uniaxial LC medium

For the case of birefringent liquid crystals in Figure 6.1, the principal x'-axis is parallel to $\vec{n}$, and hence we obtain

$$\varepsilon_{x'} = \varepsilon_{\parallel}; \tag{6.2}$$

$$\varepsilon_{y'} = \varepsilon_{z'} = \varepsilon_{\perp}; \tag{6.3}$$

$$n_{x'} = n_{\parallel} = n_e; \tag{6.4}$$

$$n_{y'} = n_{z'} = n_{\perp} = n_0, \tag{6.5}$$

where the refractive index for the ordinary beam is n_0 and for the extraordinary beam n_e according to Equations (2.3) and (2.4). Two values of the dielectric constants and of the refractive indices are respectively equal, which defines a uniaxial system. Birefringent liquid crystals are uniaxial. If all three values in the pairs of Equations (6.2) (6.3) and (6.4) (6.5) are different, the medium is biaxial. The medium is isotropic if all three values are equal.

The problem to be solved is outlined in Figure 6.1. The given incident light with wave vector k_i gives rise to reflected light with wave vector k_r and, as we shall see, to the refracted ordinary beam with k_0 and the extraordinary beam with k_e. In this chapter, we shall determine the nature of the ordinary and extraordinary beams which, according to Maxwell's equations, can propagate through the LC cell. The derivation is based on Yeh (1988) and Zeile (2001).

The Jones vectors of the electric and magnetic planar and harmonic field are

$$\vec{E} = E e^{i(\omega t - \vec{k}\vec{r})} \tag{6.6}$$

$$\vec{H} = H e^{i(\omega t - \vec{k}\vec{r})} \tag{6.7}$$

with the components in the x', y' and z'-coordinates $E_\nu e^{i(\omega t - \vec{k},\vec{r}_\nu)}$ and $H_\nu e^{i(\omega t - \vec{k},\vec{r}_\nu)}$, $\nu = x'$, y' and z'. We start with Maxwell's equations

$$rot\,\vec{E} = \nabla x \vec{E} = -\frac{\partial \mu \vec{H}}{\partial t} \tag{6.8}$$

and

$$rot\,\vec{H} = \nabla x \vec{H} = \frac{\partial \varepsilon \vec{E}}{\partial t} = \frac{\partial \vec{D}}{\partial t}, \tag{6.9}$$

where $\vec{D} = \varepsilon \vec{E}$ stands for the electrical displacement and $\nabla x\, \vec{E}$ for

$$\nabla x \vec{E} = \begin{pmatrix} x'_0 & y'_0 & z'_0 \\ \frac{\partial}{\partial x'} & \frac{\partial}{\partial y'} & \frac{\partial}{\partial z'} \\ E_{x'} & E_{y'} & E_{z'} \end{pmatrix}. \tag{6.10}$$

x'_0, y'_0 and z'_0 are the unity vectors in the x', y' and z' directions in Figure 6.1.

Substitution for $\vec{E}$ and $\vec{H}$ from Equations (6.6) and (6.7), respectively, into Equations (6.8) and (6.9) yields

$$\vec{k}\, x\, \vec{E} = \omega \mu \vec{H} \tag{6.11}$$

and

$$\vec{k}\, x\, \vec{H} = -\omega \varepsilon\, \vec{E} = -\omega \vec{D}. \tag{6.12}$$

It is interesting to note from Equation (6.12) that the wave vector $\vec{k}$ is always perpendicular to $\vec{D}$. Only if ε is a scalar is it also perpendicular to $\vec{E}$. In the general case of birefringence, ε is a tensor, and hence k is in general no longer perpendicular to $\vec{E}$.

Inserting $\vec{H}$ in Equation (6.11) into Equation (6.12) provides

$$\vec{k}\, x(\vec{k}\, x \vec{E}) + \omega^2 \mu\, \varepsilon\, \vec{E} = 0. \tag{6.13}$$

Calculating the principal axes x', y' and z' in Figure 6.1 with ε in Equation (6.1) translates Equation (6.13) into

$$\begin{pmatrix} \omega^2 \mu \varepsilon_{x'} - k_{y'}^2 - k_{z'}^2 & k_{x'} k_{y'} & k_{x'} k_{z'} \\ k_{x'} k_{y'} & \omega^2 \mu \varepsilon_{y'} - k_{x'}^2 - k_{z'}^2 & k_{y'} k_{z'} \\ k_{x'} k_{z'} & k_{y'} k_{z'} & \omega^2 \mu \varepsilon_{z'} - k_{x'}^2 - k_{y'}^2 \end{pmatrix} \begin{pmatrix} E_{x'} \\ E_{y'} \\ E_{z'} \end{pmatrix} = 0. \tag{6.14}$$

This equation exhibits only nontrivial solutions if the determinant vanishes, resulting, with Equations (6.1), (6.4) and (6.5), with the wave vector in vacuum $k_{vac}=(\omega/c)$ from Equation (3.9) and c in Equation (3.3), in

$$\begin{vmatrix} k_{vac}^2 n_e^2 - k_{y'}^2 - k_{z'}^2 & k_{x'}k_{y'} & k_{x'}k_{z'} \\ k_{x'}k_{y'} & k_{vac}^2 n_0^2 - k_{x'}^2 - k_{z'}^2 & k_{y'}k_{z'} \\ k_{x'}k_{z'} & k_{y'}k_{z'} & k_{vac}^2 n_0^2 - k_{x'}^2 - k_{y'}^2 \end{vmatrix} = 0. \tag{6.15}$$

A longer but straightforward calculation finally leads to

$$\left(\frac{k^2}{n_0^2} - k_{vac}^2\right)\left(\frac{k_{y'}^2 + k_{z'}^2}{n_e^2} + \frac{k_{x'}^2}{n_0^2} - k_{vac}^2\right) = 0, \tag{6.16}$$

where

$$k^2 = k_{x'}^2 + k_{y'}^2 + k_{z'}^2. \tag{6.17}$$

The first solution of Equation (6.16) is

$$k^2 = n_0^2 k_{vac}^2 = k_0^2 = k_{0x'}^2 + k_{0y'}^2 + k_{0z'}^2. \tag{6.18}$$

This is the square of the wave vector k_0 of the ordinary beam, as it depends only upon $n_0=n_\perp$. Due to Equation (6.18), k_0 lies on a sphere with radius $n_0\, k_{vac}$, as shown in the cross-section in Figure 6.2(a).

The second solution of Equation (6.16) provides the extraordinary beam

$$k_e = k_{ex'}x_0' + k_{ey'}y_0' + k_{ez'}z_0' \tag{6.19}$$

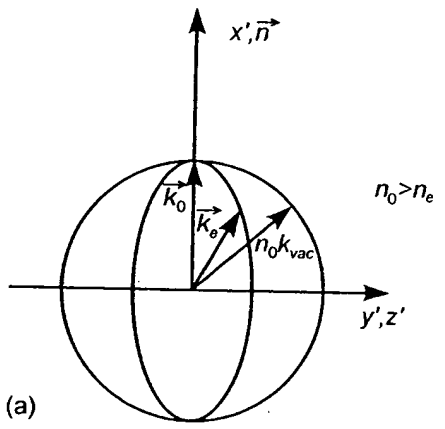

Figure 6.2 Cross-sections through the sphere of k_0 and the ellipsoid of revolution of k_e for (a) $n_0>n_e$, (b) $n_0<n_e$

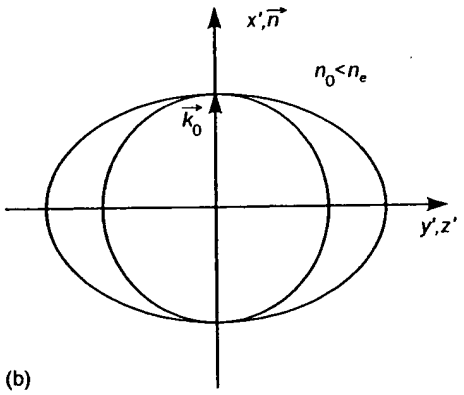

Figure 6.2 (continued)

as

$$\frac{k_{ey'}^2 + k_{ez'}^2}{n_e^2} + \frac{k_{ex'}^2}{n_0^2} = k_{vac}^2. \tag{6.20}$$

This represents an ellipsoid of revolution, depicted for $n_0 > n_e$ in Figure 6.2(a) and for $n_0 < n_e$ in Figure 6.2(b).

The vector $\vec{E}_0$ belonging to $\vec{k}_0$ is obtained by inserting Equation (6.18) into Equation (6.14), resulting with Equations (6.1), (6.6) and (3.9) in

$$\begin{array}{rcrcrcl} \left(k_{vac}^2\left(n_e^2 - n_0^2\right) + k_{0x'}^2\right)E_{x'} & + & k_{0x'}k_{0y'}E_{y'} & + & k_{0x'}k_{0z'}E_{z'} & = & 0 \\ k_{0x'}k_{0y'}E_{x'} & + & k_{0y'}^2 E_{y'} & + & k_{0y'}k_{0z'}E_{z'} & = & 0. \\ k_{0x'}k_{0z'}E_{x'} & + & k_{0y'}k_{0z'}E_{y'} & + & k_{0z'}^2 E_{z'} & = & 0 \end{array} \tag{6.21}$$

Due to the singular coefficient matrix as demonstrated in Equation (6.15), the solution to Equations (6.21) depends upon an arbitrary constant C_0, and is

$$\vec{E}_0 = C_0(k_{0z}\, y_{0'} - k_{0y} z_{0'}). \tag{6.22}$$

Obviously, $\vec{E}_0$ lies in the $y_{0'} - z_{0'}$-plane, and hence $\vec{E}_0 \perp x_{0'}$ or $\vec{E}_0 \perp \vec{n}$ holds. In Figure 6.1, only one vector $\vec{E}_0$ of the possible vectors in the plane perpendicular to $\vec{n}$ is drawn. As a consequence of its direction, $\vec{E}_0$ only experiences the scalar permittivity $\varepsilon_\perp$, from which it follows that $\vec{k}_0 \perp \vec{E}_0$, as depicted in Figure 6.1. This $\vec{k}_0$ is also drawn in Figure 6.1. The unity vector O_0 in the direction of $\vec{E}_0 \perp \vec{k}_0$ and $\vec{E}_0 \perp \vec{n}$ is given by

$$O_0 = \frac{\vec{k}_0 \times \vec{n}}{|\vec{k}_0 \times \vec{n}|}. \tag{6.23}$$

The dielectric displacement $\vec{D}_0 = \varepsilon_\perp \vec{E}_0$ is parallel to $\vec{E}_0$.

The wave vector k_e of the extraordinary beam is derived from the second solution in Equation (6.16) defined by

$$\frac{k_{ey}^2 + k_{ez}^2}{n_e^2} + \frac{k_{ex}^2}{n_0^2} - k_{vac}^2 = 0. \tag{6.24}$$

For the determination of k_e, we assume a (so far) unknown angle Θ_e between $\vec{n}$ and $\vec{k}_e$, as shown in Figure 6.1. From this follows, for the components of k_e,

$$k_{ex'} = k_e \cos\Theta_e \tag{6.25}$$

and

$$k_{ey'}^2 + k_{ez'}^2 = k_e^2 \sin^2\Theta_e, \tag{6.26}$$

and hence for Equation (6.24),

$$k_e^2\left(\frac{\sin^2\Theta_e}{n_e^2} + \frac{\cos^2\Theta_e}{n_0^2}\right) = k_{vac}^2. \tag{6.27}$$

We introduce an effective refractive index

$$n_f = \frac{k_e}{k_{vac}} \tag{6.28}$$

and insert it into Equation (6.27), leading to

$$\frac{\sin^2\Theta_e}{n_e^2} + \frac{\cos^2\Theta_e}{n_0^2} = \frac{1}{n_f^2} \tag{6.29}$$

or

$$\left(\frac{n_f \sin\Theta_e}{n_e}\right)^2 + \left(\frac{n_f \cos\Theta_e}{n_0}\right)^2 = 1 \tag{6.30}$$

or

$$n_f = \frac{n_0 n_e}{\sqrt{n_0^2 \sin^2\Theta_e + n_e^2 \cos^2\Theta_e}}. \tag{6.31}$$

The ellipsoid of revolution in Equation (6.30) with the axis $n_f \sin\Theta_e$ and $n_f \cos\Theta_e$ is depicted in Figure 6.3(a).

This effective index of refraction will greatly simplify investigations of anisotropic media by treating the propagation of light with an angle Θ to $\vec{n}$ with a refractive index n_f in Equation (6.31), and with

$$k_e = n_f k_{vac}, \tag{6.32}$$

Figure 6.3 (a) extraordinary b

as depicted in index $n_0 = n_\perp$. $\vec{E}_e$ is deter coefficient ma

where $E_{ex'}$ is a Another for

where k_{vac}^2 in I The equatio

n

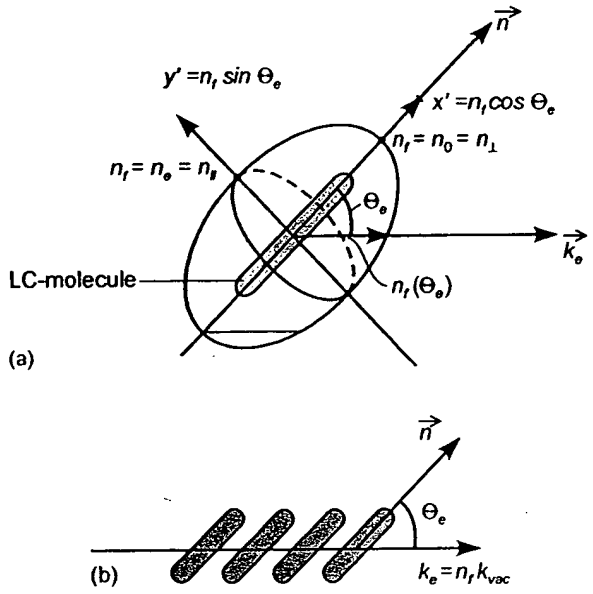

Figure 6.3 (a) The ellipsoid of revolution representing n_f in Equation (6.30); (b) propagation of the extraordinary beam obliquely through LC molecules

as depicted in Figure 6.3(b). The light with the wave vector k_0 provides the second refractive index $n_0 = n_\perp$.

$\vec{E}_e$ is determined by inserting Equation (6.24) into Equation (6.14) with the singular coefficient matrix in the form of Equation (6.15). The solution is

$$E_{ey'} = -\frac{k_{ex'}k_{ey'}}{k_{ey'}^2 + k_{ez'}^2}\left(\frac{n_e}{n_0}\right)^2 E_{ex'}, \tag{6.33}$$

$$E_{ez'} = -\frac{k_{ex'}k_{ez'}}{k_{ey'}^2 + k_{ez'}^2}\left(\frac{n_e}{n_0}\right)^2 E_{ex'}, \tag{6.34}$$

where $E_{ex'}$ is a free constant, as the determinant in Equation (6.15) is zero.

Another form of this solution is obtained by starting with

$$n_f = \frac{k_e}{k_{vac}} = \left(\frac{k_{ex'}^2 + k_{ey'}^2 + k_{ez'}^2}{((k_{ey'}^2 + k_{ez'}^2)/n_e^2) + (k_{ex'}^2/n_0^2)}\right)^{1/2}, \tag{6.35}$$

where k_{vac}^2 in Equation (6.24) was used.

The equation

$$\frac{n_f^2 - n_0^2}{n_0^2 n_e^2} = \frac{n_f^2}{n_0^2 n_e^2} - \frac{1}{n_e^2} = \frac{k_{ex'}^2 + k_{ey'}^2 + k_{ez'}^2}{n_0^2 n_e^2\left(((k_{ey'}^2 + k_{ez'}^2)/n_e^2) + (k_{ex'}^2/n_0^2)\right)} - \frac{1}{n_e^2}$$

where Equation (6.35) was used, yields

$$\frac{n_f^2 - n_0^2}{n_0^2} = \frac{(n_e^2 - n_0^2)(k_{ey'}^2 + k_{ez'}^2)}{n_0^2(k_{ey'}^2 + k_{ez'}^2) + n_e^2 k_{ex'}^2} + \frac{1}{n_e^2}. \tag{6.36}$$

Similarly, we obtain

$$\frac{n_f^2 - n_e^2}{n_0^2} = \frac{(n_0^2 - n_e^2)k_{ex'}^2}{n_0^2(k_{ey'}^2 + k_{ez'}^2) + n_e^2 k_{ex'}^2} + \frac{1}{n_0^2}, \tag{6.37}$$

from which

$$\frac{n_f^2 - n_e^2}{n_f^2 - n_0^2} = -\left(\frac{n_e}{n_0}\right)^2 \frac{k_{ex'}^2}{k_{ey'}^2 + k_{ez'}^2} \tag{6.38}$$

follows. With Equation (6.38), Equations (6.33) and (6.34) assume the form

$$E_{ey'} = \frac{k_{ey'}}{k_{ex'}} \frac{n_f^2 - n_e^2}{n_f^2 - n_0^2} E_{ex'} \tag{6.39}$$

and

$$E_{ez'} = \frac{k_{ez'}}{k_{ex'}} \frac{n_f^2 - n_e^2}{n_f^2 - n_0^2} E_{ex'}. \tag{6.40}$$

$E_{ex'}$ can be chosen as a free constant. For reasons of symmetry, we choose

$$E_{ex'} = C_e \frac{k_{ex'}}{n_f^2 - n_e^2}, \tag{6.41}$$

with the arbitrary constant C_e yielding

$$\vec{E}_e = C_e \left(\frac{k_{ex'}}{n_f^2 - n_e^2} x_{0'} + \frac{k_{ey'}}{n_f^2 - n_0^2} y_{0'} + \frac{k_{ez'}}{n_f^2 - n_0^2} z_{0'} \right). \tag{6.42}$$

The pertinent electric displacement is $\vec{D}_e = \varepsilon \vec{E}_e = \vec{d}_{e0} D_e$, where ε is the tensor in Equation (6.1) and d_{e0} is the unity vector in the direction of $\vec{D}_e$. According to Equation (6.12), $\vec{D}_e \vec{k}_e = 0$ always holds. On the other hand, for $\vec{E}_e \vec{k}_e$ we obtain, with Equations (6.39) and (6.40), and the components of k_e,

$$\vec{E}_e \vec{k}_e = E_{ex'} k_{ex'} \left(1 - \frac{n_e^2}{n_0^2}\right) \neq 0, \tag{6.43}$$

indicating that $\vec{E}_e$ is not perpendicular to $\vec{k}_e$. For conventional LC materials, $|1 - (n_e^2/n_0^2)|$ lies between 0.1 and 0.2. Therefore, the difference in the directions of $\vec{k}_e$ and $\vec{E}_e$ is relatively small. The plane for $\vec{E}_e$ almost perpendicular to $\vec{k}_e$ is shown in Figure 6.1.

We determine the unity vector e_0 in

$$\vec{E}_e = e_0 E_e. \tag{6.44}$$

In Yeh (1988), the approximation $e_0 \approx d_{e0}$ is used, whereas the exact solution is derived from $\vec{E}_e = \varepsilon^{-1}\vec{D}_e$ for (Zeile, 2001)

$$e_0 = \frac{\varepsilon^{-1}\vec{D}_e}{|\varepsilon^{-1}\vec{D}_e|}. \tag{6.45}$$

The total solution consisting of the ordinary and extraordinary beam is

$$E_{tot} = \vec{E}_0 e^{-\vec{k}_0\vec{r}} + \vec{E}_e e^{-\vec{k}_e\vec{r}}. \tag{6.46}$$

For the direction of $\vec{E}_0$ and $\vec{E}_e$, only the planes in which these vectors lie can be obtained. The specific direction in these planes is obtained by investigating the propagation of the incident light with wave vector $\vec{k}_i$ in the LC medium. This task will not be treated here; solutions can be found in Yeh (1988). We shall only briefly outline the steps taken for solving the problem. First, we have to satisfy the boundary conditions for the tangential components for the electrical field of the incident and the reflected light for the pertinent wave vectors outside the LC medium and for the field and the wave vectors of the ordinary and extraordinary beams inside the medium. Then, the known solutions for $\vec{k}_0$, $\vec{E}_0$, $\vec{k}_e$ and $\vec{E}_e$ with the free constants C_0 and C_e provide special solutions for $\vec{E}_0$ and $\vec{E}_e$ in their planes in Figure 6.1. The inclusion of the reflected beam leads to 2×2 matrices instead of the column matrices for the field used so far (Berreman, 1972).

6.2 Enhancement of the Performance of LC Cells

6.2.1 The degradation of picture quality

So far we have investigated the optical properties of an LC cell viewed perpendicularly to the glass plates. An oblique viewing direction is given by the azimuth angle ϕ and the off-axis angle Θ_e in Figure 6.4. As a rule, the larger Θ_e becomes, the more the optical performance is degraded. There is a loss of contrast and a grey level inversion, especially in the lower and upper vertical directions, as well as a change in colour for larger angles ϕ. A typical conoscopic image of an LCD, in which the contrast is plotted versus the two angles in Figure 6.4, is shown in Figure 6.5 (Haas, 1999). Characteristic curves for a display indicate where the contrast decreases below 10 : 1, and where a grey shade inversion takes place. The meaning of a grey level inversion is explained in Figure 6.6, where the lower level of luminance $g8$ becomes brighter than the next brighter level $g7$ (Haas, 1999). A feature degrading with increasing Θ_e is the fairly equal spacing of the grey scales with equal steps in voltage V_{LC}. Thus, grey shade performance is dependent upon Θ_e and is obviously poor on the right side of Figure 6.6. Measures against degraded contrast and the associated colour

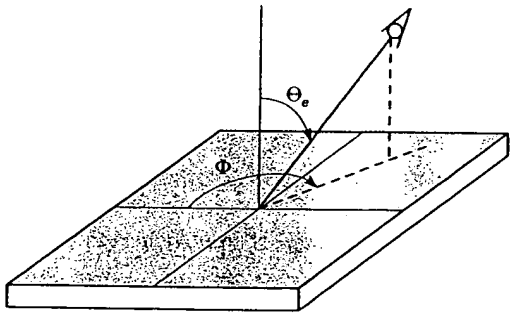

Figure 6.4 Viewing direction defined by azimuth angle Φ and off-axis angle Θ_e

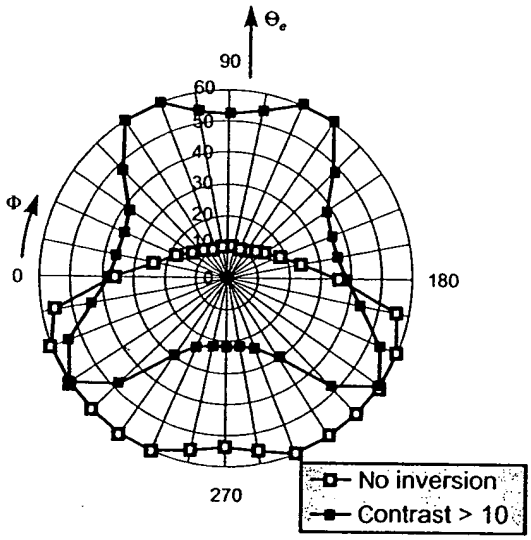

Figure 6.5 Curves of isocontrast and of limit for grey shade inversion of an LCD

changes for an increased viewing angle are compensation foils with negative birefringence, adding an inverse cell with negative or positive birefringence and the in-plane switching mode (IPS); the grey scale inversion is avoided by multi-domain pixels, IPS and by foils with positive birefringence (Haas, 1999; Yeh and Gu, 1999).

6.2.2 *Optical compensation foils for the enhancement of picture quality*

The enhancement of contrast

Crucial for the enhancement of contrast over a wide viewing angle is the improvement of the black state. In vertically aligned LCDs such as the DAP cell with crossed polarizers in the field-off state, or the TN cell with crossed polarizers in the field-on state, there is an

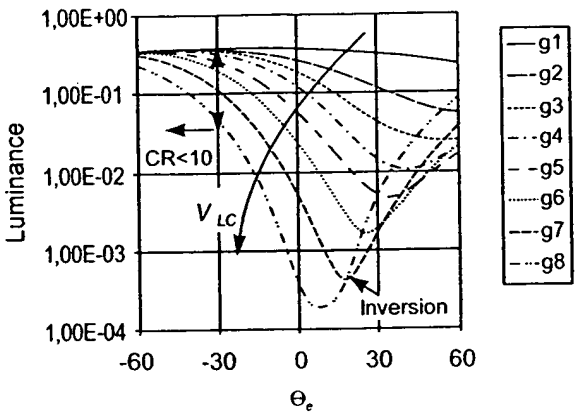

Figure 6.6 Grey level inversion versus Θ_e in the picture of an LCD

excellent black state independent of λ and d only when viewed in the vertical direction, for which the optical retardation is zero. When viewed under an oblique angle Θ_e, as depicted in Figure 6.7, the retardation is

$$\Delta n_f d_0 = (n_f(\Theta_e) - n_0)d_0 \neq 0, \tag{6.47}$$

with n_f in Equation (6.31) and d_0 standing for the effective cell thickness. The index ellipsoid in Figure 6.3(a) with $\vec{n}$ as the axis of revolution is drawn for one LC molecule in Figure 6.7, exhibiting a positive birefringence $\Delta n = n_e - n_0 > 0$. This is true for nematic LC materials.

We obtain a cigar-shaped index ellipsoid. Because of the non-vanishing retardation in Equation (6.47), the observer does not see a perfect black state at an angle Θ_e. Some light leaks through spoiling the black state. This leakage can be suppressed by adding a negative retardation to $\Delta n_f d_0$ in Equation (6.47) (Eblen *et al.*, 1994). This is achieved by a foil with a

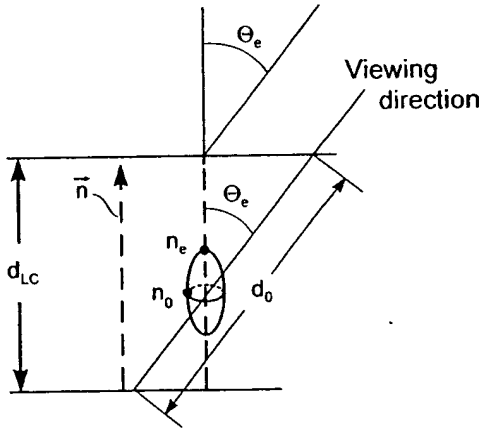

Figure 6.7 Optical retardation for oblique viewing angle $\Theta_e \neq 0$

negative birefringence due to the indexes $n'_e < n'_0$, as shown in Figure 6.8. The optical retardation along the viewing path in Figure 6.8 is required to be

$$\Delta n_f d_0 + \Delta n'_f d'_0 \approx 0, \tag{6.48}$$

with $\Delta n'_f = n'_f(\Theta) - n'_0 < 0$ for the negative birefringence foil in Figure 6.8 with a pancake-shaped index ellipsoid. This shape may be realized by discotic liquid crystals, as mentioned in Chapter 2, from which the term *discotic foils* is derived.

A homogeneous and uniaxial birefringent plate with the optical axis perpendicular to the surface of the plate is called a c-plate. In Figure 6.8, the liquid crystal is a positive and the discotic film a negative c-plate.

The compensation in Equation (6.48) works from $\Theta_e = 0$ up to a fairly large angle around $\Theta_e = 60°$. This is demonstrated by the 10 : 1 isocontrast curves in Figure 6.9(a) for an ECB cell with and without a discotic compensation film. The range without grey inversion has also been widened, as depicted in Figure 6.9(b). Left and right viewing symmetry is improved by placing one discotic film of half the thickness on each side of the LCD cell, as depicted schematically in Figure 6.10. The improved symmetry of contrast and limit of grey shade inversion is demonstrated in Figure 6.11 for the ECB cell of Figures 6.9(a) and (b). Discotic films do not add retardation in the vertical viewing direction as is desired for a good black state in this direction.

Compensation foils for LC molecules with different optical axes

The compensation discussed so far was based on vertically aligned LC molecules in Figure 6.7. In TN cells, however, the molecules close to the two orientation layers stay aligned with directors parallel to the surface of the glass plates and perpendicular to each other. Also, the optical retardation of these layers has to be compensated by negative birefringence, with discotic layers the directors of which are also parallel to the surface and perpendicular to

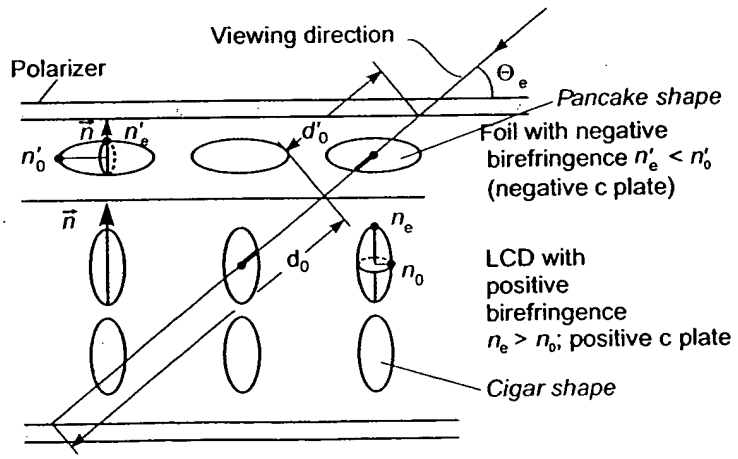

Figure 6.8 Compensation of retardation with a negative c plate

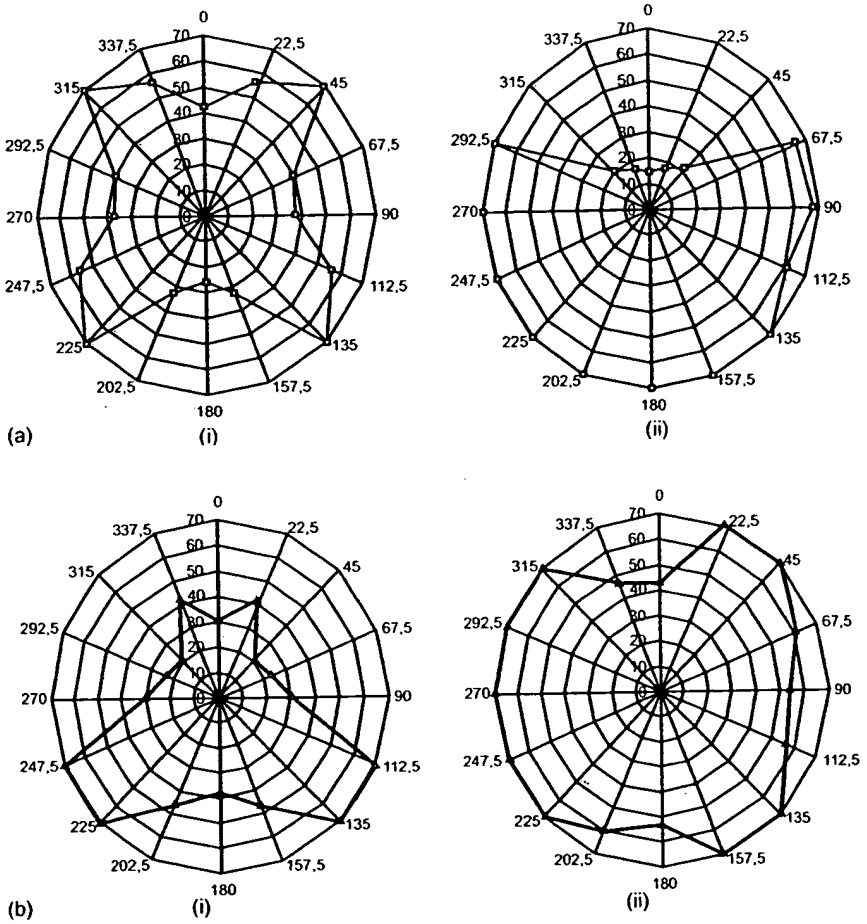

Figure 6.9 (a) A 10:1 isocontrast curve for an ECB cell with (ii) and without (i) a discotic compensation film (Haas, 1999); (b) the limit curves of grey inversion in an ECB cell with (ii) and without (i) a discotic film

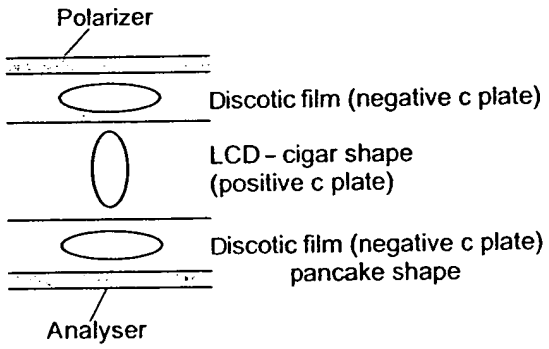

Figure 6.10 Discotic films of half thickness on either side of LCD

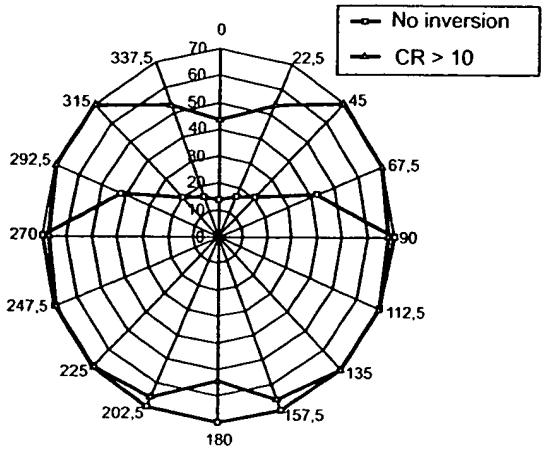

Figure 6.11 Symmetrical curves for 10:1 isocontrast and for limit of grey inversion of cell in Figures 6.9(a) and 6.9(b)

each other. This compensation is done individually on each side of the LCD. Figure 6.12 depicts this compensation scheme schematically (Eblen *et al.*, 1994). The compensation layer with the optical axis parallel to the surface of the layer is called an *a-plate*. In all the compensation foils introduced so far, the directors are either parallel or perpendicular to the plane of the polarizer. In that way, however, the retardation of molecules with an optical axis oblique to the plane of the polarizer cannot be compensated. To achieve this, a negatively birefringent foil with an optical axis parallel to the oblique axis of the molecules is required. Such a homogeneous negatively birefringent plate is called a *negative o-plate*. Solutions have been proposed by Eblen *et al.* (1997) and Witte *et al.* (1999). An alternative is the film introduced by Fuji (Mori *et al.*, 1997). According to Figure 6.13, the configuration of the

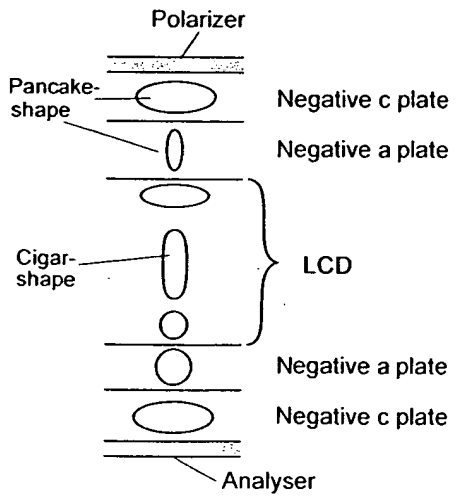

Figure 6.12 Compensation of the retardations of the midlayer and surface layer molecules

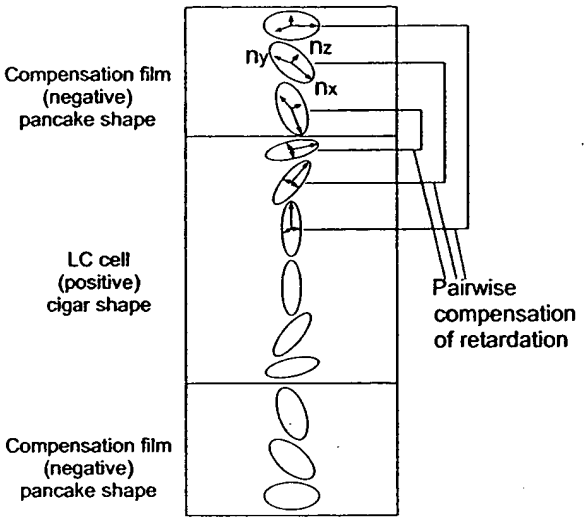

Figure 6.13 The compensation of retardations of an LCD by discotic films with the same direction of optical axes

molecules of an LCD in the black state is repeated with parallel optical axes by the molecules of a negatively birefringent discotic film, for the known reasons of symmetry, with half the thickness on either side of the LCD. The molecules compensate each other pair-wise, as indicated in Figure 6.13. Had we the same number of molecules in the two discotic films and in the LCD, we would obtain a perfect compensation. As a rule, the number of molecules in the discotic film is smaller, but it still produces very good compensation. The vertical viewing direction inherently still exhibits a very good black state. Losses in the films render the display a little darker. The result is demonstrated by the isocontrast curve and the limit for grey scale inversion shown in Figure 6.14.

The black state of TN cells viewed perpendicular to the glass plates can be improved again by a pair-wise compensation but this time with a positively birefringent compensation film (Scheffer and Nehring, 1998). This is shown in Figure 6.15, in which a TN-LCD is followed by a second non-addressed TN-LCD cell. This set-up is mainly used for STN cells, and is called a Double STN Cell (DSTN). The uppermost molecule in the second cell is rotated by 90° with respect to the lowermost molecule in the first cell. Furthermore, the twists in the two cells are opposite. Otherwise, the configuration is the same. The operation is explained by recalling from Equations (2.10), (2.11) and (2.12) that the speed of propagation of light is larger if the E-field encounters a smaller index of refraction. For $n_{\parallel} > n_{\perp}$ we have a fast and a slow axis of propagation, as shown in the top view on the molecules in Figure 6.15. The speeds add up pair-wise to an equal speed $V_{\text{fast}} + V_{\text{slow}}$ in both directions if the pairs are chosen, as indicated by equal numbers, in Figure 6.16. As a consequence, the non-addressed pixels of both displays form an isotropic path for light incident perpendicularly to the glass plates. This results in a perfect black state independent of the wavelength, and hence is free of any coloration. For the addressed pixel on the right-hand side of Figure 6.15, the linearly polarized light reaches the output of the upper cell unchanged, and is rotated by the lower cell towards the crossed analyser. The cell appears white.

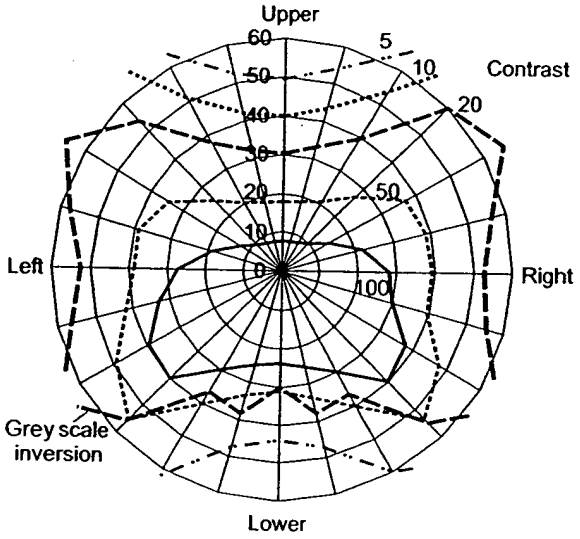

Figure 6.14 Isocontrast and limit for grey inversion after compensation with discotic films in Figure 6.13

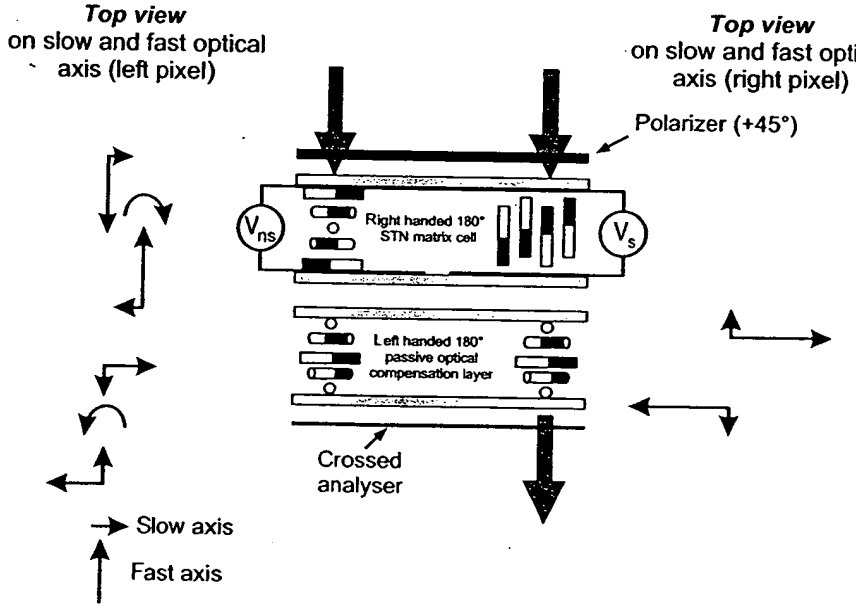

Figure 6.15 Double layer STN cell for compensation of black state and colouration and top view on slow and fast propagation axis

As a rule, the second cell is replaced by a compensation foil which, however, contains only a few layers, mostly two or three, of molecules. This is an acceptable approximation to the exact solution.

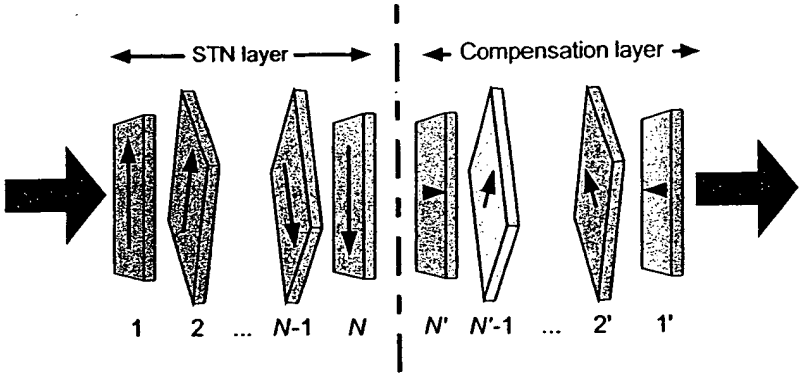

Figure 6.16 The pairs of STN layers with opposite twist for compensation in Figure 6.15

6.2.3 *Suppression of grey shade inversion and the preservation of grey shade stability*

The grey shade inversion and the grey shade stability in Figure 6.6 is related to the minima of luminance shifting to lower viewing angles with increasing voltage V_{LC}. The aim of the compensation is to shift the minima to such large angles that they are out of the viewing range. This places grey shade inversions out of view, and preserves the fairly equal spacing of the grey shades below the minima over the entire viewing range.

To understand the compensation method, we first have to grasp the cause for the minima, which is explained in Figure 6.17 for a TN cell seen in a plane perpendicular to the glass substrates. The larger the voltage V_{LC}, the smaller becomes the angle Θ_e of the midlayer molecules. The optical retardation is lowest for the viewing direction along the director of the midlayer tilt, because the E-field mainly encounters the index $n_0 < n_e$. A low optical retardation causes the polarized optical wave to twist only slightly, resulting in a small amount of light being transmitted by the crossed analyser. To the right and to the left of the direction

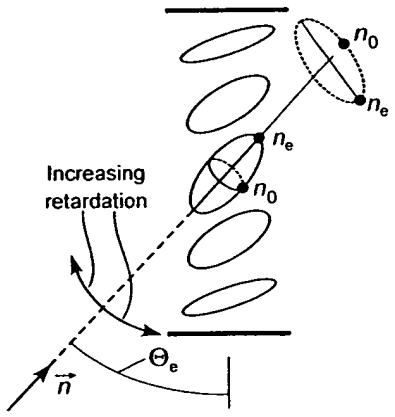

Figure 6.17 Viewing direction for minimum luminance

parallel to the director $\vec{n}$ of the midlayer, the index increases, resulting in increasing retardation and luminance. The lowest retardation can be compensated by adding a positively birefringent layer with its optical axis perpendicular to the optical axis of the midlayer molecules, as shown with dotted lines in Figure 6.17. This positively birefringent compensation layer with an optical axis oblique to the surface of the glass plates is called a *positive 0-layer*. For the compensation, a medium tilt of the midlayer of 45° is chosen; the optical axis of the 0-plate is then at 45° to the glass plates (Yeh and Gu, 1999). For reasons of symmetry, this axis also lies in the y-z-plane of Figure 4.1. To preserve the viewing performance perpendicular to the glass plates ($\Theta_e = 0$), we have to avoid adding optical retardation in this direction by inserting a positive a-plate with its optical axis perpendicular to the 0-plate, as already encountered as an alternative to the Fuji film mentioned earlier. As a result, the minima of the luminance can be shifted for most practical applications out of the viewing range.

6.2.4 Fabrication of compensation foils

Positively bi-refringent a-plates are fabricated by stretching uniaxial polymer films such as polyvinyl alcohol (PVA); a-plates with a negative birefringence consist of uniaxially aligned discotic materials such as triphenylene derivates. Polymer films with a homeotropic alignment of nematic LC materials form positively birefringent c-plates; c-plates with a negative birefringence are fabricated by pressing uniaxially oriented polymer films with random azimuthal angles, by spin-coated polyimide films, or by using homeotropically oriented discotic compounds. Finally, stratified media consisting of isotropic thin layers with alternating different refractive indices are birefringent, and may be used for c-plates with the optical axes perpendicular to the layer interfaces. The thickness of the layers has to be much smaller than the wavelength of the light used. This effect is called form birefringence (Yeh and Gu, 1999).

6.3 Electro-optic Effects with Wide Viewing Angle

So far we have investigated viewing angle limitation and problems with grey shades in TN cells. The key issue in those cells is the minimum luminance for a viewing direction parallel to the director of the tilted mid-layer molecules. This is a basic cause for all the shortcomings of a display associated with an oblique viewing direction. These shortcomings do not show up in displays with multidomain pixels, in non-twisted displays such as displays with In-Plane Switching (IPS) or in a π cell, which is also called a cell with bend-alignment or an Optically Compensated Bend cell (OCB cell).

6.3.1 Multidomain pixels

A further means to suppress inversion and maintain grey shade stability whilst enhancing the viewing angles for which the contrast ratio exceeds 10:1 is the use of multidomain pixels, as shown in Figure 6.18 for the case of four domains in each pixel (Yang, 1991; Iimura and Kobayoshi, 1994). These domains possess two different surface tilts combined with two different twist senses of rotation for the helixes. Let us consider one of the helixes and the

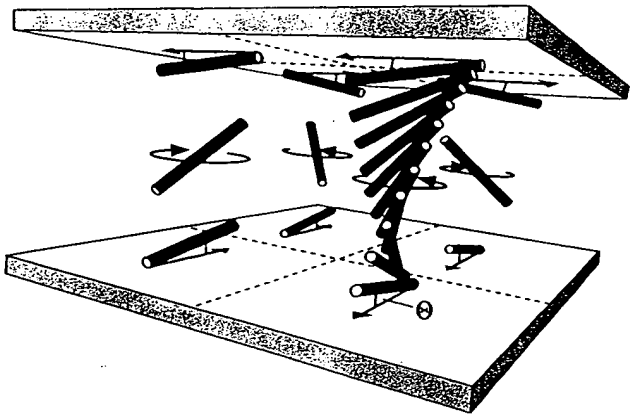

Figure 6.18 A pixel with four domains

direction of the mid-layer tilt at which, as explained in Figure 6.17, a minimum luminance occurs. In this direction, the luminances of the other three helixes do not exhibit their minimum. Therefore, the entire pixel does not generate a minimum luminance in this direction. This is true for all three remaining directions with minimized luminance of the other helixes in a pixel. As a result, the point of low luminance has been shifted to larger angles Θ_e. This effect, we already know, results in avoiding inversion, in maintaining grey shade stability and additionally in enhancing the viewing angle.

The use of more than four domains does not lead to a noticeable improvement, whereas two domains also work, but not so efficiently as four domains.

The alignment of the domains with an adjustable tilt angle on the orientation layer is achieved by a Linear Photo-Polymerization (LPP) (Schadt *et al.*, 1996; Schadt, 1999) of polyvinyl 4-methoxy cinnamate photopolymer with UV-radiation. Liquid crystal alignment occurs as shown in Figure 6.19, at the intersection of the surface of the photopolymer with

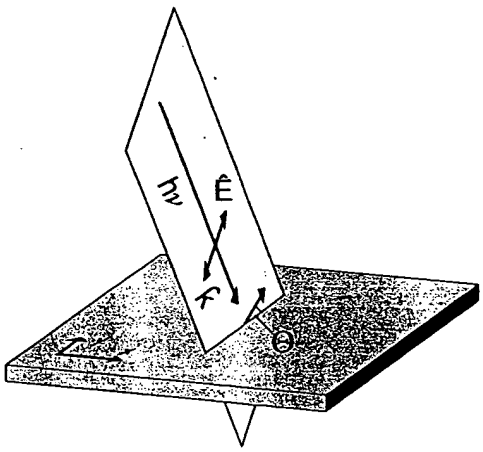

Figure 6.19 The photo-induced alignment and adjustment of the tilt angle Θ of LC molecules on top of the orientation layer

the plane defined by the wave vector $\vec{k}$ and the vector of the E-field of the radiation. The tilt angle Θ depends upon the angle of incidence of $\vec{k}$, and can be adjusted in the entire range $\Theta \in [0, \pi/2]$.

6.3.2 In-Plane switching

In the IPS mode, the directors of the molecules remain at all times parallel to the surface of the glass plates, as outlined in Figure 6.20 (Oh-e *et al.*, 1995). They are rotated by an electric field applied parallel to the glass plates between the two electrodes in each pixel. This rotation generates grey shades similar to the operation of a Fréedericksz cell in Section 3.2.1.

The normally black cell works as follows: in the field-free state in Figure 6.20, the LC molecules are oriented by the orientation layer all in parallel to the direction of the polarizer. Hence, the incoming linearly polarized light does not experience birefringence, reaches the back plate with an unchanged polarization, and is thus blocked in the crossed analyser, as in the Fréedericksz cell. If an electric field is applied, the LC molecules rotate and tend to align parallel to the field. The molecules anchored on the orientation layer and in its vicinity do not rotate, resulting in a twist angle dependent on the distance z in Figure 6.20. Only for a large electric field are all the molecules rotated parallel to the field independent of z besides two thin layers on top of the orientation layers. For this configuration, a straightforward calculation with Jones vectors provides the transmission T through the crossed analyser as

$$T = \frac{1}{2} \sin 2\beta \sin^2 \gamma, \tag{6.49}$$

with the retardation $\gamma = (2\pi/\lambda)\Delta nd$ and the twist angle β of the molecules from the field-free state. The largest transmission $T = 1/2$ is reached for $\gamma = \pi/2$ and $\beta = \pi/4$. In the field-free state with $\beta = 0$, we obtain $T = 0$.

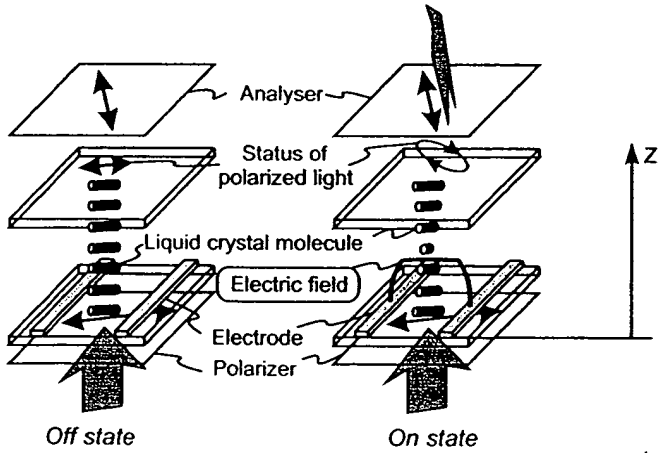

Figure 6.20 Principle of the in-plane switching mode

Parallel polarizers define the normally white mode. The big advantage of the IPS mode is the previously mentioned absence of a minimum in transmission for an oblique viewing angle. This absence, as previously provided by compensation foils or by mulitdomain pixels, is now offered by a different optical system, with widened viewing angles as demonstrated in Figure 6.21. The fact that the directors of the LC molecules are always parallel to the plane of the polarizers suppresses, for all viewing angles, the damaging effect of tiltet molecules in Figure 6.17 and in Equation (6.31) on the viewing angle. Therefore, IPS belongs to the LCDs with the best viewing characteristics. Two shortcomings of IPS also have to be mentioned, even though work to remedy them is under way. The two electrodes in the pixels shrink the aperture ratio to about 40 percent. The torque needed for the rotation of the molecules in plane is larger than for rotating them perpendicular to the plane, as stronger intermolecular forces have to be overcome. Therefore, response time is increased to 60 ms at $V_{LC}=7$ V, too slow for TV pictures.

6.3.3 *Optically compensated bend cells*

This cell is the same as the π cell, the fast switching of which was introduced in Section 3.2.7. Besides fast switching, the OCB cell also exhibits a wide viewing angle (Bos and Rahman, 1993; Yomaguchi, Miyashita and Uchida, 1993). Before we embark on this, we have to complete Equation (3.98) for the retardation R by including the refractive index n_f in Equation (6.29). This index applies if light propagates at an angle Θ_e to the director, as shown in Figures 6.22(a) and (b) for the known configuration of the directors in a non-addressed π cell. The retardation for on-axis viewing in Figure 6.22(a) is, with Equations (3.98) and (3.100),

$$R = \int_{z=0}^{d} \Delta n(z)dz = \int_{z=0}^{d} (n_f(\Theta_e(z)) - n_0)dz, \tag{6.50}$$

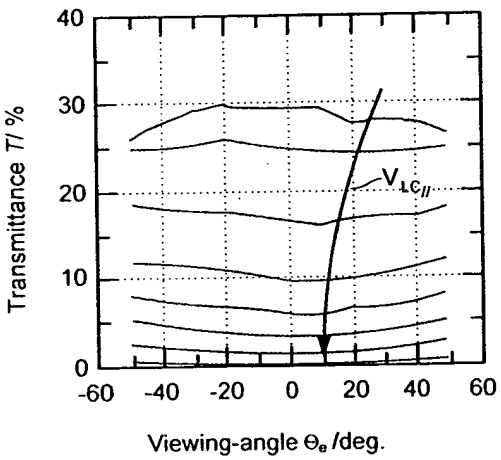

Figure 6.21 Transmittance of various grey levels versus the off-axis Θ_e for an IPS display

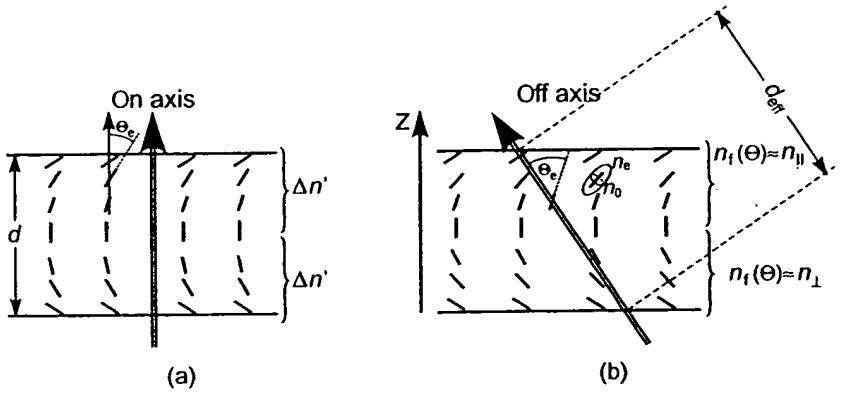

Figure 6.22 The self-compensation of the retardation R of light propagating at an oblique angle through the π-cell, (a) Light propogation in the direction of the cell normal; (b) propagation at an oblique angle

with n_f in Equation (6.29) and $\Theta_e(z)$ the angle changing with z in Figure 6.22. The π cell is a $\lambda/2$ plate,yielding

$$R = \frac{\pi}{2} = \int_{z=0}^{d} (n_f(\Theta_e(z)) - n_0)dz, \tag{6.51}$$

from which the thickness d can be calculated if $n_f(\Theta_e(z))$ is known. With Equation (3.101), an effective anisotropy Δn_{eff} is introduced, yielding

$$R = \Delta n_{\text{eff}}\, d = \int_{z=0}^{d} (n_f(\Theta_e(z)) - n_0)dz \quad \text{or}$$

$$\Delta n_{\text{eff}} = \frac{1}{d}\int_{z=0}^{d} (n_f(\Theta_e(z)) - n_0)dz. \tag{6.52}$$

As a rule, the integrals are evaluated numerically. The retardation for the viewing under the oblique angle in Figure 6.22(b) is

$$R = \int_{z=0}^{d_{\text{eff}}} (n_f(\Theta_e(z)) - n_0)dz. \tag{6.53}$$

The aim is to shift this retardation as close to $\pi/2$ in Equation (6.51) as possible, which renders the viewing under angle Θ_e equal to the viewing perpendicularly.

In the lower portion of the cell, $n_f(\Theta_e)$ in Equation (6.53) is close to $n_f = n_0 = n_\perp$ as $\Theta_e \approx 0$ in Equation (6.29), and in the upper portion $n_f(\Theta_e)$ is close to $n_f = n_e = n_\parallel > n_\perp$ as $\Theta_e \approx \pi/2$. So the excess retardation in the upper portion is compensated by the smaller retardation in the lower portion. This self-compensation of the π cell shifts R in Equation (6.53) close to $R = \pi/2$ in Equation (6.51), which expands the viewing range considerably as an inherent property of the π cell. The isocontrast curve of a π cell is contained in Figure 6.23 (Bos and

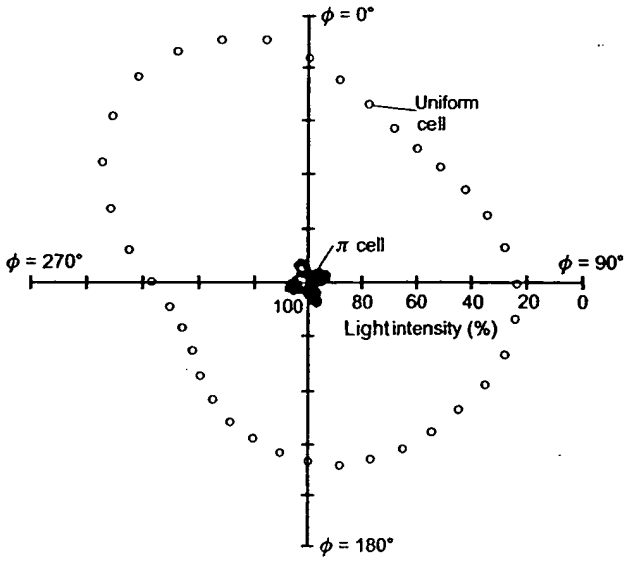

Figure 6.23 Isocontrast curves of a π cell

Koehler, 1984). The viewing angle can be further enhanced by adding a negatively birefringent compensation foil with the self-compensating director configuration (Bos and Rahman, 1993). This renders the π cell one of the most interesting LCDs.

6.4 Polarizers with Increased Luminous Output

The issue of increasing the luminance of LC cells that use polarized light is also of some urgence. A linear polarizer allows only 50 percent of the light to pass, the *s*-wave, because it has to absorb the remaining 50 percent of the light, the *p*-wave, which is polarized perpendicular to the *s*-wave. Two 'loss-less' polarizers which recycle the otherwise lost *p*-wave have been developed. They enhance luminance.

It is worth mentioning a further effect of polarizers which can reduce the viewing angle of a display. The two orthogonal axes of a polarizer for the *s*-wave and *p*-wave no longer appear orthogonal if viewed from an oblique angle. This causes leakage of light from the *p*-wave thus spoiling the black state and the grey shades for larger viewing angles.

6.4.1 A reflective linear polarizer

The 3M company (Wortman, 1907) has developed the reflective polarizer shown in Figure 6.24, which consists of a three layer laminate. Each layer contains an isotropic and a birefringent film. The refractive indices for the ordinary beam in the birefringent film and for the isotropic film are equal. Thus, the stack of layers is isotropic for linearly polarized light in the direction of the ordinary beam. This beam can pass. The complimentary beam polarized in the direction of the extraordinary beam is reflected if the periodicity of the stack and the wavelength are matched. The reflected polarized light is again reflected by a

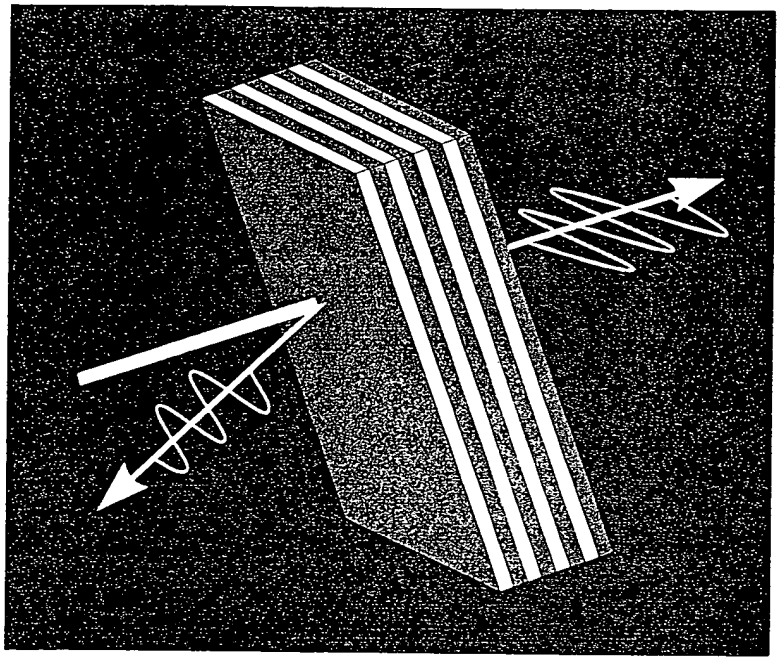

Figure 6.24 The three-layer laminate of the 3M reflective polarizer

depolarizing diffuser, upon which this light is again treated the same way as the previous incoming beam. This transmission and reflection of beams is repeated until, theoretically, all the light has been transmitted in linear polarization. Measurements reveal that practically 85 percent instead of 50 percent of the light is transformed into a linear polarization state, reflecting in a 70 percent gain in luminance.

6.4.2 *A reflective polarizer working with circularly polarized light*

The Merck company (Coates *et al.*, 1996) introduced the reflective polarizer shown in Figure 6.25, in which unpolarized light is incident on a birefringent foil with a helical molecular structure like in an STN display. The helical structure is generated by a cholesteric film. The helix only allows light circularly polarized in the opposite sense of the helix to pass. The light circularly polarized in the same sense as the helix is reflected. This is shown in the stages 1 and 2 in Figure 6.25. The reflected light incident on the diffuser is depolarized by scattering (stage 3 in Figure 6.25). The component with a circular polarization in the opposite direction as the helix is transmitted, whereas the reflected component undergoes depolarization by scattering. This play is repeated indefinitely. The circular polarization at the output of the cholesteric film is transformed into a linear polarization by a $\lambda/4$-plate, as discussed in Section 5.2. Finally, a linear polarizer suppresses spurious portions of the *p*-wave which has leaked through. This solution is able to deliver 80 percent of the incoming light into the LC cell.